A gene regulatory network controlled by *VvbHLH105*/*VvHSP20-31*/*VvENO2* during H_2O_2-promoted fruit ripening in grape

Jia-Lin Xing [1,2], Jia-Qi Xu [3], Ke-Ying Duan [1,2], Ding-Ding Zuo [3], San-Jun Liu [4], Shi-Ping Cheng [5], Arif Atak [6], Justin G Lashbrooke [7], Da-Long Guo [1,2*]

[1]College of Horticulture and Plant Protection, Henan University of Science and Technology, Luoyang, 471023, China

[2]Henan Key Laboratory of Germplasm Innovation and Utilization of Eco-economic Woody Plant, Henan University of Science and Technology, Luoyang, 471023, China

[3]College of Agriculture, Henan University of Science and Technology, Luoyang, 471023, China

[4]Zhengzhou Fruit Research Institute, CAAS, Zhengzhou, 450009, China

[5]School of Chemical and Environmental Engineering, Pingdingshan University, Pingdingshan，467000, China

[6]Department of Horticulture, Faculty of Agriculture, Bursa Uludağ University, Bursa, 16059, Türkiye

[7]Department of Genetics, Stellenbosch University, Stellenbosch 7600, South Africa

[*]For correspondence (e-mail guodalong@haust.edu.cn)

ACCEPTED MANUSCRIPT

© The Author(s) 2026. Published by Oxford University Press on behalf of the Nanjing Agricultural University. This is an Open Access article distributed under the terms of the Creative Commons Attribution License https://creativecommons.org/licenses/by/4.0/, which permits unrestricted reuse, distribution, and reproduction in any medium, provided the original work is properly cited.

Downloaded from academic.oup.com/hr/advance-article/doi/10.1093/hr/uhag485/9097232 by Bursa Uludag University user on 19 November 2026

Abstract

Small heat shock proteins (sHSPs) play pivotal roles in stress responses and plant growth. However, their functions in fruit ripening are not fully understood. Here, we investigated the molecular basis of exogenous hydrogen peroxide (H_2O_2)-promoted grape berry ripening. *VvHSP20-31* was significantly down-regulated following H_2O_2 treatment. Yeast one-hybrid and two-hybrid library screening identified its upstream transcription factor basic helix-loop-helix 105 (VvbHLH105) and interacting protein enolase 2 (VvENO2). The transient transformations in grape berries plus additional stable transformations in tomato and *Arabidopsis* all demonstrate that *VvbHLH105*, *VvHSP20-31*, and *VvENO2* negatively regulate fruit ripening. H_2O_2 treatment reduced the transcription of the *VvbHLH105*, *VvHSP20-31*, and *VvENO2* genes in grape berries. This suppression not only promoted the expression of ripening-related genes, but also elevated the level of endogenous H_2O_2. These results were further validated in tomato and *Arabidopsis*. Additionally, H_2O_2 treatment inhibited the protein interaction of VvHSP20-31 and VvENO2. This study elucidates a molecular mechanism by which HSP20 regulates grape berry ripening through *VvbHLH105*-mediated transcriptional activation and VvENO2 protein interaction, offering valuable insights into exogenous H_2O_2 promoting grape berry ripening.

Key words: grape, berry ripening, HSP20, hydrogen peroxide, bHLH, ENO2

ACCEPTED MANUSCRIPT

Downloaded from academic.oup.com/hr/advance-article/doi/10.1093/hr/uhag485/9097232 by Bursa Uludag University user on 19 November 2026

Introduction

Grape (*Vitis vinifera* L.) is an economically significant fruit tree globally, boasting both high nutritional and cultural value. The berry of the grape, in its various forms, whether fresh, dried, or processed into wine and raisins, forms the basis for a wide range of industries and offers significant nutritional and health benefits [1]. Fruit ripening is a complex process that is regulated by a combination of external environmental and intrinsic developmental signals [2–5]. Early ripening is among the most important characteristics desired in fruit crops [6–8]. Early ripening fruits arrive on the market earlier, meeting consumers' early demand for these fruits. In many grape breeding programs, earliness is among the desired and targeted selection criteria [9].

Reactive oxygen species (ROS) play a key role in fruit ripening by regulating the antioxidant system [10, 11]. For example, reactive oxygen species initiate the senescence process of fruit ripening through the accumulation of O_2^- and H_2O_2 [12, 13]. ROS promote the degradation of cell wall polysaccharides, leading to fruit softening and thus accelerating fruit ripening and senescence [14]. H_2O_2 functions as an oxidizing agent as an exogenous reactive oxygen species, but has detrimental effects on components of the surrounding biological system in case of excessive accumulation [15]. However, at low concentrations, H_2O_2 can act as a signaling molecule and is instrumental in the process of fruit ripening. For example, some changes are observed in the composition of antioxidants during ripening of tomato fruit, while there is a significant oxidative burst and rapid H_2O_2 accumulation during grape ripening [16]. This is reported to be associated with softening and ripening [17]. Pears have an increase in antioxidant capacity during storage, which extends their storage life [18]. Spraying 300 mmol/L H_2O_2 in 'Kyoho' grape variety 25 days after flowering could promote berry ripening 20 days earlier [19]. To further analyze the transcriptome data of H_2O_2 treatment at different developmental periods, RNA-seq and RT-qPCR results revealed that *VvHSP20-31* gene was significantly differentially expressed in the treated groups compared with the control group, and it was also hypothesized that

ACCEPTED MANUSCRIPT

Downloaded from academic.oup.com/hr/advance-article/doi/10.1093/hr/uhag485/9097232 by Bursa Uludag University user on 19 November 2026

the *VvHSP20-31* gene plays an important role in grape berry ripening [20].

Heat stress proteins (HSPs) play a crucial role in the response of plants to environmental stressors, as well as in their growth and development process [21]. HSPs are categorized by molecular weight into HSP100s, HSP90s, HSP70s, HSP60s, and small molecular weight heat stress proteins (sHSPs) [22]. In certain plant tissues, HSP20s account for the largest proportion of HSPs. HSP20 acts as an ATP-independent molecular chaperone against various stresses, including oxidative stress, by re-establishing normal protein conformation and intracellular homeostasis [23]. The HSP20 protein could balance the ROS concentration by protecting the conformation and activity of ROS scavenging proteins [24, 25]. sHSPs play pivotal roles in stress responses, plant growth and fruit ripening. For example, the overexpression of *OsHSP16.9* in rice confers thermotolerance [26]. Similarly, overexpression of *LeHSP21* in tobacco boosts antioxidant capacity [27]. In rice, some HSP20s are expressed in almost all tissues, suggesting the possibility that HSP20s may act as housekeeping genes to regulate normal plant growth and developmental processes [28]. *SlHSP17.4* is expressed at almost all stages of tomato fruit development and reaches high levels when ripening [29]. Notably, *SlHSP21* is known to protect Photosystem II (PSII) from oxidative stress and concurrently promotes color transition during fruit ripening, underscoring its critical function in this process [30]. However, the role of HSP20s in grape berry ripening is not yet known.

Enolase (ENO, 2-phospho-Dglyceratehydrolyase), also known as 2-phospho-D-glycerate hydrolase, is able to catalyse the conversion of 2-phospho-D-glycerate (2-PGA) to phospho-enolpyruvate (PEP) [31]. Recent studies have revealed that, beyond its canonical role in glycolysis, ENO2 exerts pivotal functions in plant growth, tolerance to abiotic stresses, and the regulation of fruit size. It has been demonstrated that *Arabidopsis* ENO2^{-} mutants have shorter primary roots in the primordium, fewer numbers of lateral roots, and smaller cotyledons with more dwarfed above-ground parts [32]. H_2O_2 contributes to the cold hardiness of *Arabidopsis* by facilitating the sulfenylation of *AtENO2*

ACCEPTED MANUSCRIPT

Downloaded from academic.oup.com/hr/advance-article/doi/10.1093/hr/uhag485/9097232 by Bursa Uludag University user on 19 November 2026

[33]. A promoter variant of *SlENO2* in tomato is associated with a significant increase in fruit size [34]. However, the function of ENO2 in grape berry development and ripening is unclear and needs to be explored more deeply.

bHLH (basic/helix-loop-helix) transcription factors contain a basic helix-loop-helix structure and are widely present in eukaryotes with many members [35]. Some bHLH proteins have been shown to bind to sequences containing a consensus core element called the E box (5′-CANNTG-3′), with the G box (5′-CACGTG-3′) being the most common form [36]. bHLH transcription factors play a role in regulating fruit ripening [37]. *bHLH14* is involved in regulating the expression of genes related to carotenoid synthesis and promotes kiwifruit ripening [38]. *MabHLH28* positively regulates the expression of softening genes and promotes banana fruit ripening [39]. The up-regulation of *SlbHLH95* resulted in higher sensitivity to ethylene, leading to an increased accumulation of total carotenoids, and accelerating the early ripening of tomato fruits [40]. *MdbHLH3* helped to regulate the expression of apple softening-related enzymes also accelerated fruit softening and ripening [41]. However, the functions of bHLH in grape berry ripening are not known.

In this study, we investigated the molecular basis of exogenous H_2O_2-promoted grape berry ripening, focusing on a regulatory module involving *VvHSP20-31*, an H_2O_2-responsive gene that negatively regulates ripening. Yeast-based library screening assay, the upstream transcription factor VvbHLH105 and the interacting protein VvENO2 were identified. The binding of VvbHLH105 to the *VvHSP20-31* promoter was verified by Y1H, dual-luciferase reporter, and electrophoretic mobility shift assay (EMSA), while the VvHSP20-31–VvENO2 interaction was confirmed by Y2H and GST pull-down, etc. Notably, the expression of these genes was inversely associated with endogenous H_2O_2 levels and ripening-related gene expression. Collectively, our findings provide insights into the regulating mechanism of exogenous H_2O_2 on grape berry ripening.

ACCEPTED MANUSCRIPT

Downloaded from academic.oup.com/hr/advance-article/doi/10.1093/hr/uhag485/9097232 by Bursa Uludag University user on 19 November 2026

Results

Identification of the H_2O_2-responsive *VvHSP20-31* gene in grape

Sequence analysis showed that the full length of *VvHSP20-31* coding sequence was 483 bp, encoding 160 amino acids (Table S1). Phylogenetic tree analysis revealed that *VvHSP20-31* had high homology with *RcHSP20* and *OsHSP20* (Fig. 1A). The expression pattern of *VvHSP20-31* was investigated in five tissues and six berry developmental periods of 'Kyoho' grapes [11]. As showed that *VvHSP20-31* was most highly expressed at the K2 period of berry development, and was lowly expressed in the tissues of root, stem, leaf, tendril and inflorescence (Fig. 1B). With berry development, the expression of *VvHSP20-31* was down-regulated at the berry veraison stage (K5). Overall, this result suggests that *VvHSP20-31* may be a negative regulator of berry ripening. Protein sequence analysis identified *VvHSP20-31* as containing the HSP20 structural domain (α-crystallin domain, ACD) and belonging to the small heat stress protein family members (Fig. 1C; Fig. S1A). The analysis of cis-acting elements in the promoter identified several binding sites specific to transcription factors, as well as elements responsive to light, hormones, and stress. This suggests that *VvHSP20-31* could be regulated by transcription factors and involved in multiple physiological processes (Fig. 1D; Fig. S1B). Subcellular localization analysis revealed that *VvHSP20-31* located in the nucleus and cytoplasm (Fig. 1E and F). Additionally, the promoter activity of *VvHSP20-31* was analyzed, confirming that its promoter possesses transcriptional activation activity and remains unaffected by H_2O_2 (Fig. S1C). The above results suggest that *VvHSP20-31* is associated with grape berry ripening.

VvHSP20-31 negatively regulates fruit ripening

To further verify the regulatory role of *VvHSP20-31* during grape fruit ripening, we constructed the pIR-*VvHSP20-31*-OE overexpression vector and the silencing vector pIR-*VvHSP20-31*-RNAi, for transiently overexpressing and silencing *VvHSP20-31* in grape

ACCEPTED MANUSCRIPT

Downloaded from academic.oup.com/hr/advance-article/doi/10.1093/hr/uhag485/9097232 by Bursa Uludag University user on 19 November 2026

berries, respectively and the pIR empty vector was used as the control. Plasmids pIR-*VvHSP20-31*-OE, pIR-*VvHSP20-31*-RNAi, and the pIR empty vector were transiently transformed into distinct grape clusters on the different vine. This procedure was conducted over three separate intervals: 32 days (June 12, 2024), 39 days (June 19, 2024), and 46 days (June 26, 2024) after the flowering of the 'Kyoho' grape variety. Observations of the berry were made after one week, subsequent to each transformation, accompanied by photographic documentation. Phenotypic analysis of grape bunches conducted at three distinct stages of infestation indicated that the overexpression of the *VvHSP20-31* resulted in a delayed ripening process. Conversely, silencing of the *VvHSP20-31* led to an accelerated ripening process when compared to the pIR empty-loaded infested bunches (Fig. 2A). The results of fluorescence quantification demonstrated that a transient expression system had been successfully established in grape berries (Fig. 2B).

Furthermore, we examined the expression of eight genes associated with grape berry development and ripening in transiently transformed berries [42]. *VvAG2* and *VvSEP3* encode MADS-box transcription factors associated with developmental regulation, while *VvMYBPA1* regulates proanthocyanidin biosynthesis. *VvMSA* participates in ABA signaling, and *VvHT* is associated with hexose transport. *VvCTG* and *VvGRIP4* are associated with cell-wall modification and cell expansion, whereas *VvADH2* encodes alcohol dehydrogenase 2 and is induced at the onset of ripening. Compared with controls, all eight genes were significantly downregulated in *VvHSP20-31*-overexpressing (OE) berries and upregulated in *VvHSP20-31* RNA interference (RNAi) berries (Fig. 2C). Together with the observed phenotypes, these results support a negative regulatory role for *VvHSP20-31* in grape berry ripening.

To further characterize the role of *VvHSP20-31* in climacteric fruits ripening, the coding sequence of *VvHSP20-31* was overexpressed in tomato. Three independent transgenic lines (#1, #2 and #3) were generated by assessing expression levels in plants and phenotypic observations. Consistent with our speculation, a late ripening phenotype

ACCEPTED MANUSCRIPT

Downloaded from academic.oup.com/hr/advance-article/doi/10.1093/hr/uhag485/9097232 by Bursa Uludag University user on 19 November 2026

was observed in three positive lines (Fig. 2D). The results of RT-qPCR indicated that the overexpression system was successfully established in tomato fruits (Fig. 2E). In addition, the number of days from anthesis to color change were analyzed. It demonstrated that the time to color change was delayed by 3 to 5 days in *VvHSP20-31* fruits compared with WT fruits (Fig. 2F and G). These results suggest that *VvHSP20-31* negatively regulates the ripening of climacteric fruits.

Furthermore, we conducted an overexpression of *VvHSP20-31* in *Arabidopsis*. The seeds of the transgenic *Arabidopsis* were subsequently planted on a screening medium that contained antibiotics. The majority of the *Arabidopsis* specimens did not survive, while a small number exhibited normal growth (Fig. S2A). Seeds from T3 generation transgenic *Arabidopsis* plants were harvested through monoculture and subsequently replanted. Three lines exhibiting the highest expression levels (*VvHSP20-31*-OE#1-3) were chosen for phenotypic analysis (Fig. S2B). Observations indicated that, at the early growth stage, the overexpression of *VvHSP20-31* resulted in a delay in both the bolting and flowering of the *Arabidopsis* plants, as well as a later ripening of fruit pods in comparison to the wild type (Fig. S2C). This result indicates that *VvHSP20-31* negatively regulates *Arabidopsis* fruit pod ripening.

VvbHLH105 binds to the *VvHSP20-31* promoter and activates its expression

H_2O_2 treatment resulted in the down-regulation of *VvHSP20-31*, while the promoter activity of *VvHSP20-31* was not influenced by H_2O_2 treatments (Fig. S1C), which indicted that there would be other factors functioned. To further investigate how H_2O_2 regulates *VvHSP20-31* expression, a yeast one-hybrid (Y1H) screening assay was conducted, using the *VvHSP20-31* promoter fragment (-918 bp to -1476 bp) as a bait vector, identifying VvbHLH105 (Table S2; Fig. S3A–C). Sequence analysis revealed that *VvbHLH105* encodes a protein consisting of 237 amino acids (Table S1). Phylogenetic tree analysis

ACCEPTED MANUSCRIPT

Downloaded from academic.oup.com/hr/advance-article/doi/10.1093/hr/uhag485/9097232 by Bursa Uludag University user on 19 November 2026

indicated that the clustering of *VvbHLH105* resulted in *Vitis vinifera* and *Glycine max* being grouped together, demonstrating a relatively close degree of homology (Fig. S4A). Analysis of the promoter transient action elements revealed that it has multiple regulatory elements that may be involved in the regulation of multiple physiological processes (Fig. S4B). The expression pattern of *VvbHLH105* was analyzed in five tissues and six berry development periods of 'Kyoho' grape. As shown in (Fig. 3A), *VvbHLH105* expression was highest in early berry development and lowest in leaf and inflorescence tissues. With berry development, the expression of *VvbHLH105* was down-regulated at the grape berry veraison stage. The expression of *VvbHLH105* was significantly down-regulated following H_2O_2 treatment in comparison to the control group (Fig. S4C and D). Protein sequence analysis identified *VvbHLH105* as containing the bHLH structural domain and belonging to the bHLH transcription factor family members (Fig. S4E and F). The promoter activity analysis of *VvbHLH105* showed that its promoter was repressed by H_2O_2 (Fig. 3B). Subcellular localization analysis revealed that VvbHLH105 located in the nucleus (Fig. 3C).

AlphaFold3 predicted the presence of an interaction between the bHLH binding site in the *VvHSP20-31* promoter and VvbHLH105 (Fig. 3D). To enhance the validation of their binding *in vivo*, we conducted a Y1H assay. The expression of *proVvHSP20-31*-pAbAi in conjunction with VvbHLH105-AD in co-transformed yeast facilitated growth on SD/-L-deficient medium, in contrast to the control conditions, where *proVvHSP20-31*-pAbAi combined with AD did not exhibit growth (Fig. 3E). The promoter of *VvHSP20-31* contains a G-box element (P1: -1083 bp ~ -1088 bp) (Fig. 3F). We further performed an EMSA assay on the VvbHLH105-His protein. The results showed that VvbHLH105-His specifically bound to the G-box element in the *VvHSP20-31* promoter. The intensity of the VvbHLH105 protein complex bands diminished progressively as the concentrations of competing probes increased. In contrast, no complex bands were detected in the presence of competing probes when biotin-labeled mutant probes (where CACGTG was altered to

ACCEPTED MANUSCRIPT

Downloaded from academic.oup.com/hr/advance-article/doi/10.1093/hr/uhag485/9097232 by Bursa Uludag University user on 19 November 2026

ACATGT) were introduced [43, 44]. These findings strongly support the idea that the VvbHLH105-His protein binds specifically to the *VvHSP20-31* promoter through the G-box recognition sequence. To examine the transcriptional regulation of *VvHSP20-31* by *VvbHLH105*, we conducted a dual luciferase promoter assay. We constructed a fusion of the *VvHSP20-31* promoter region with the pGreenllo800-LUC vector, resulting in the *proVvHSP20-31*-LUC construct. Additionally, we fused the CDS of *VvbHLH105* to the pSAK277 vector, yielding the pSAK-VvbHLH105 construct (Fig. 3G). The results indicated that the co-expression of pSAK-VvbHLH105 and *proVvHSP20-31*-LUC resulted in a significantly higher relative fluorescence intensity and LUC activity in comparison to the control pSAK+*proVvHSP20-31*-LUC (Fig. 3H and I). Therefore, these results indicate that VvbHLH105 up-regulates *VvHSP20-31*, and H_2O_2 further reduces the expression of *VvHSP20-31* by inhibiting the transcription of *VvbHLH105* through its promoter.

Identification of VvENO2 as the VvHSP20-31 interacting partner

To gain more insight into the potential mechanisms of *VvHSP20-31* regulates berry ripening, we performed a yeast two-hybrid (Y2H) screening assay to identify potential interacting proteins of VvHSP20-31. As a result, an enolase protein named VvENO2 was identified in the Y2H screening library (Fig. 4A; Fig. S5A–C; Table S3). Sequence analysis showed that VvENO2 encodes 444 amino acids. Phylogenetic tree analysis revealed that *VvENO2* had high homology with *HbENO* (Fig. S6A). The analysis of promoter transient action elements revealed that it has several regulatory elements such as light response, hormone induction, and drought stress, suggesting that *VvENO2* may be involved in the regulation of multiple physiological processes (Fig. S6B). Furthermore, we conducted an analysis of the promoter activity of *VvENO2*, and the findings indicated that its promoter exhibits transcriptional activation activity (Fig. S6C). The expression pattern of *VvENO2* in five tissues and six berry development periods of 'Kyoho' grapes was analyzed and found that *VvENO2* was most lowly expressed in the tissues of stem and leaf. With berry

ACCEPTED MANUSCRIPT

Downloaded from academic.oup.com/hr/advance-article/doi/10.1093/hr/uhag485/9097232 by Bursa Uludag University user on 19 November 2026

development, the expression of *VvENO2* was down-regulated at the berry veraison and ripening stages (Fig. 4B). Protein sequence analysis identified *VvENO2* as containing two relatively conserved structural domains and belonging to members of the enolase family (Fig. S6D and E). Further analysis examined the effect of H_2O_2 treatment on *VvENO2* expression. Our findings indicated that the expression of *VvENO2* was significantly down-regulated following H_2O_2 treatment in comparison to the control group (Fig. 4C and D). Subcellular localization analysis revealed that VvENO2 is located in the nucleus and cytoplasm (Fig. 4E and F).

VvENO2 physically interacts with the VvHSP20-31

AlphaFold3 predicted the existence of an interaction between VvHSP20-31 and VvENO2 (Fig. 5A). To assess the interaction between VvHSP20-31 and VvENO2, we conducted point-to-point validation experiments utilizing the yeast two-hybrid system. The full-length cDNA of *VvHSP20-31* was ligated to the DNA-binding domain (BD) within the pGBKT7 vector, while the full-length cDNA of VvENO2 was linked to the activation domain (AD) in the pGADT7 vector. Yeast cells co-expressing VvHSP20-31-BD and VvENO2-AD demonstrated growth on a yeast medium deficient in four nutrients (SD/-T/-L/-H/-A), thereby confirming the interaction between the two proteins (Fig. 5B). We constructed the VvHSP20-31-nLUC and VvENO2-cLUC vectors to verify the interaction *in vivo* between VvHSP20-31 and VvENO2 (Fig. 5C). The results showed that both VvHSP20-31-nLUC and VvENO2-cLUC exhibited distinct fluorescent signals, and LUC activity was also increased (Fig. 5D and E). In addition, the results of GST pull-down assay indicated that VvENO2 fused with His tag was about 50~60 kDa, and the electrophoretic bands by SDS-PAGE after purification conformed to the theoretical size (Fig. S7A). VvHSP20-31 fused with GST tag was about 40~50 kDa, and the electrophoretic bands by SDS-PAGE after purification conformed to the theoretical size (Fig. S7B). Using an anti-GST antibody, the VvHSP20-31 protein was found in both the VvENO2+VvHSP20-31 eluate and its control

ACCEPTED MANUSCRIPT

Downloaded from academic.oup.com/hr/advance-article/doi/10.1093/hr/uhag485/9097232 by Bursa Uludag University user on 19 November 2026

group (unwashed). In contrast, with anti-His antibodies, the VvENO2 protein was detected in the VvENO2+VvHSP20-31 eluate and the positive control (unwashed), but not in the negative control (washed) GST+ENO2. These findings demonstrate that VvENO2 interacts with VvHSP20-31, while no interaction occurs between VvENO2 and the GST empty tag protein (Fig. 5F). Bimolecular fluorescence complementation (BiFC) assays confirmed that VvHSP20-31 and VvENO2 interact in the cytoplasm (Fig. 5G).

VvbHLH105 negatively regulates grape berry ripening

To elucidate the function of *VvbHLH105* in grape ripening, we engineered an overexpression construct (pIR-*VvbHLH105*-OE) and a hairpin RNAi silencing vector (pIR-*VvbHLH105*-RNAi). These constructs were transiently transformed into grape clusters, with the pIR empty vector serving as the control. Three infiltrations were performed on distinct grape bunches from the different vine at 31 DAF (June 10, 2025), 38 DAF (June 17, 2025), and 45 DAF (June 24, 2025). Phenotypic evaluation of berries at 7 days post-infiltration revealed that *VvbHLH105*-overexpressing clusters exhibited delayed veraison transition, whereas RNAi-silenced clusters showed accelerated ripening compared to controls (Fig. 6A), indicating *VvbHLH105* acts as a negative ripening regulator. RT-qPCR analysis confirmed successful transient transformation efficacy (Fig. 6B). By measuring the quantitative ripening indicators in grape berries, it was found that compared with the control, the anthocyanin and soluble solids content in pIR-*VvbHLH105*-RNAi grape berries were increased, whereas they decreased in pIR-*VvbHLH105*-OE berries (Fig. S8A and B). In addition, gene expression analysis showed that, compared with the control group, ripening-related genes were significantly up-regulated in the *VvbHLH105*-RNAi berry clusters but down-regulated in the overexpression clusters (Fig. 6C). Collectively, these results indicate *VvbHLH105* as a negative regulator of grape berry ripening.

To further clarify the function of *VvbHLH105*, *VvHSP20-31*, and *VvENO2* in the

ACCEPTED MANUSCRIPT

Downloaded from academic.oup.com/hr/advance-article/doi/10.1093/hr/uhag485/9097232 by Bursa Uludag University user on 19 November 2026

regulation of berry ripening, we employed both a transient silencing system and an overexpression system *in vitro* in ripening grape berries. Specifically, we utilized gene silencing and overexpression vectors, namely *VvbHLH105*-RNAi, *VvbHLH105*-OE, *VvHSP20-31*-RNAi, *VvHSP20-31*-OE, *VvENO2*-RNAi, and *VvENO2*-OE, which were introduced into grape berries. An pIR empty vector was utilized as a control in this experiment. The RT-qPCR assay demonstrated that *VvbHLH105* functions upstream of *VvHSP20-31*, thereby enhancing the expression of *VvHSP20-31*. Furthermore, transient overexpression or silencing of either *VvHSP20-31* or *VvENO2* altered the transcript level of the other gene, suggesting a potential association between their expression levels (Fig. 6D and E).

VvENO2 negatively regulates fruit ripening

In order to investigate the regulatory role of *VvENO2* in grape ripening, the overexpression vector pIR-*VvENO2*-OE and the silencing vector pIR-*VvENO2*-RNAi were developed and subsequently transiently introduced into grape clusters, with the pIR empty vector serving as a control. Phenotypic observation of grape clusters at three periods of infestation revealed that a delayed ripening process was observed after overexpression of the *VvENO2* and an accelerated ripening process was observed after silencing of the *VvENO2* compared with the control (Fig. 7A). This demonstrated the negative regulatory role of *VvENO2* in the grape ripening process. The results of RT-qPCR indicated that the transient expression system was successfully established in grape berries (Fig. 7B). Additionally, we examined the expression levels of ripening-related genes within *VvENO2* transgenic grape berries. Relative to the control group, these genes demonstrated a marked up-regulation in pIR-*VvENO2*-RNAi grape berries, whereas a significant down-regulation was noted in pIR-*VvENO2*-OE grape berries (Fig. 7C). These findings imply that *VvENO2* functions as a negative regulator of grape ripening.

Similarly, overexpression of the *VvENO2* in tomato produced 3 independent

ACCEPTED MANUSCRIPT

Downloaded from academic.oup.com/hr/advance-article/doi/10.1093/hr/uhag485/9097232 by Bursa Uludag University user on 19 November 2026

transgenic lines (#4, #5 and #9). Consistent with previous results, a late-ripening phenotype was observed in the three positive lines (Fig. 7D). The results of RT-qPCR indicated that the overexpression system was successfully established in tomato fruits (Fig. 7E). In addition, we found that the time to fruit veraison was delayed by 3 to 5 days in *VvENO2* over expressing fruits compared with WT fruits (Fig. 7F and G). These results suggest that *VvENO2* negatively regulates the ripening of climacteric fruits. Overexpression of *VvENO2* in *Arabidopsis* was screened, and seeds from the T3 generation of transgenic *Arabidopsis* were harvested through monoculture and subsequently replanted (Fig. S9A). The three lines with the highest expression (*VvENO2*-OE#1-3) were selected for phenotypic observation (Fig. S9B). It could be seen at the early growth stage that, after overexpression of *VvENO2,* the *Arabidopsis* exhibited delayed ripening of fruit pods in comparison to the WT (Fig. S9C). This finding suggests that *VvENO2* exerts a negative regulatory effect on the ripening of fruit pods in *Arabidopsis*.

VvbHLH105, *VvHSP20-31*, and *VvENO2* influence H_2O_2 levels of fruit

To further investigate the link between *VvbHLH105*, *VvHSP20-31*, and *VvENO2* regulation of berry ripening and H_2O_2, grape berries were transiently transformed with *VvbHLH105*, *VvHSP20-31*, and *VvENO2*. Subsequently, sections of the transformed berries were stained with DAB. Additionally, leaves from transgenic tomato plants that overexpress these genes, as well as leaves from overexpressing transgenic *Arabidopsis thaliana*, were subjected to DAB staining individually. It was observed that grape berry sections exhibiting transient silencing of *VvHSP20-31* displayed a darker staining compared to the control. Conversely, grape berry sections that underwent transient overexpression of *VvHSP20-31* exhibited lighter staining (Fig. 8A), similar results could be seen in grape sections that were transiently transformed with *VvENO2* and *VvbHLH105* (Fig. 8B and C), indicating an increased accumulation of H_2O_2 in grape berries that were silenced for *VvHSP20-31*, *VvENO2* and *VvbHLH105*, while a decreased accumulation of H_2O_2 was demonstrated in

ACCEPTED MANUSCRIPT

Downloaded from academic.oup.com/hr/advance-article/doi/10.1093/hr/uhag485/9097232 by Bursa Uludag University user on 19 November 2026

berries with overexpression (Fig. 8D–F). Similarly, the overexpression of *VvHSP20-31* and *VvENO2* in tomato leaves resulted in a lighter staining compared to the wild type, where the H_2O_2 content was assessed in alignment with the staining results (Fig. 8G–I). Consistent findings were also observed in *Arabidopsis* (Fig. S10A and B). These results suggest that *VvbHLH105*, *VvHSP20-31*, and *VvENO2* could influence endogenous H_2O_2 levels.

H_2O_2 weakens the VvHSP20-31–VvENO2 interaction

In our previous study, we found that H_2O_2 had a negative regulatory effect on the expression of *VvHSP20-31* [19]. Therefore, we further aimed to verify whether gene interactions respond to H_2O_2 to regulate berry ripening. Additionally, we treated tobacco with 300 mM H_2O_2 and measured malondialdehyde (MDA) content and relative electrical conductivity (REC). We found that H_2O_2 treatment did not affect cellular oxidative damage or cell viability compared to untreated controls (Fig. S11A and B).

To further observe the response of VvHSP20-31–VvENO2 interaction to H_2O_2, VvHSP20-31-nLUC and VvENO2-cLUC vectors were constructed and similarly injected into the leaf blades of *N. benthamiana*, which were subsequently treated with H_2O_2. The fluorescence intensity of VvHSP20-31-nLUC and VvENO2-cLUC was reduced by H_2O_2 treatment and was lower compared to the control (Fig. 9A and B), and LUC activity was decreased. BiFC experiments also confirmed that H_2O_2 treatment attenuated the strength of the VvHSP20-31–VvENO2 interaction (Fig. 9C). Based on these results, we further confirm that H_2O_2 attenuates the interaction between VvHSP20-31 and VvENO2. Ultimately, we elucidate the molecular mechanisms by which H_2O_2 mediates grape berry ripening (Fig. 9D).

Discussion

The molecular regulation of grape ripening involves a network that integrates external

ACCEPTED MANUSCRIPT

Downloaded from academic.oup.com/hr/advance-article/doi/10.1093/hr/uhag485/9097232 by Bursa Uludag University user on 19 November 2026

environmental factors and endogenous signaling pathways [2]. Through RNA-seq analysis of H_2O_2-treated early-ripening 'Kyoho' grapes, we observed a significant down-regulation of *VvHSP20-31* expression. The results of this study suggest that the identified genes function as negative regulators that govern the ripening process of grape berries. It should be noted that *Arabidopsis* siliques are dry fruits, which differ from grape berries (which are fleshy, non-climacteric fruits). In this study, the roles of *VvHSP20-31* and *VvENO2* in fruit ripening are primarily supported by transient transformations in grape berries and stable transformations in tomatoes. In this model, VvbHLH105 directly activates *VvHSP20-31* transcription, while VvHSP20-31 interacts with VvENO2 at the protein level. The VvbHLH105–*VvHSP20-31* branch and the VvHSP20-31–VvENO2 branch are better interpreted as two converging regulatory layers that jointly influence endogenous H_2O_2 level and fruit ripening. This study contributes to a deeper understanding of the regulatory mechanisms underlying the promotion of grape ripening by H_2O_2 treatment.

VvHSP20-31 as a negative regulator of grape berry ripening

In plants, small heat shock proteins (sHSPs) represent the most prevalent class of proteins associated with heat stress response. These proteins exhibit molecular weights that typically range from 12 to 42 kDa, which has led to their designation as HSP20s. HSPs function as molecular chaperones that mitigate various forms of stress-induced damage [45]. In our investigation, we observed that the overexpression of *VvHSP20-31* in grape, tomato, and *Arabidopsis* leaves resulted in a significant reduction of endogenous H_2O_2 levels compared to the control group. Conversely, silencing *VvHSP20-31* led to an increase in endogenous H_2O_2 content. This finding indicates an inverse relationship between *VvHSP20-31* expression and H_2O_2 accumulation, thereby suggesting its involvement in the regulation of ROS homeostasis. Further, at the K6 stage, the ripening process of the grapes is largely completed, so *VvHSP20-31* expression increases, thereby slowing down the ripening process. If the expression goes down continuously, the ripening process

ACCEPTED MANUSCRIPT

Downloaded from academic.oup.com/hr/advance-article/doi/10.1093/hr/uhag485/9097232 by Bursa Uludag University user on 19 November 2026

theoretically would not be stopped. It may be function as the molecular break at K6 stage, whose specific mechanism need to be explored in the future. This observation aligns with the established role of sHSPs in stabilising ROS scavenging enzymes [24]. Furthermore, HSP20s appear to delay fruit ripening by alleviating oxidative stress. Banana ripening is accompanied by reactive oxygen stress, which leads to oxidation of thiol-containing proteins to regulate fruit ripening. As well as up-regulation of protein expression of HSPs and differential accumulation of eight HSPs transcripts [46]. The induction of gene silencing through RNA interference targeting *SlHSP17.7* has been shown to postpone the ripening process of tomato fruit [47]. The observed down-regulation of *VvHSP20-31* during the ripening process of the grape berry, along with its inhibitory effect on ripening-related genes such as *VvAG2* and *VvADH2*, aligns with similar findings reported in tomato and banana species. These results indicate that HSP20 plays a significant role in the regulation of plant growth, development, and ripening. In contrast to S*lHSP17.7* in tomato, which inhibits ripening via ethylene signaling, *VvHSP20-31* may function through a distinct H_2O_2-dependent mechanism, indicating species-specific regulatory differences [13]. The localization of VvHSP20-31 in both the nucleus and cytoplasm suggests that it may fulfil various roles within plant cells, warranting further investigation into its functions during berry development.

VvbHLH105 plays a pivotal transcriptional regulatory role linking H_2O_2 to ripening

Members of the bHLH transcription factor family possess two conserved yet functionally distinct structural domains: the amino-terminal basic DNA-binding domains (E-box and G-box) and the carboxy-terminal HLH domain. Both structural domains play a critical role in the assembly of the active DNA-binding complex [48]. Recent studies have demonstrated that numerous members of the bHLH family engage in interactions with various regulatory proteins to modulate the expression of target genes [49]. This modulation plays a critical role in the regulation of plant growth and development. For

ACCEPTED MANUSCRIPT

Downloaded from academic.oup.com/hr/advance-article/doi/10.1093/hr/uhag485/9097232 by Bursa Uludag University user on 19 November 2026

instance, the formation of a ternary protein complex involving bHLH transcription factors, R2R3 MYB proteins, and WD40 repeat proteins has been shown to influence anthocyanin accumulation [50]. Our research indicates that VvbHLH105 functions as an upstream transcriptional activator of *VvHSP20-31*, thereby regulating its transcriptional expression (Fig. 3G–I). These findings expand the functional of bHLH transcription factors in the context of fruit ripening. The expression levels of *SlbHLH95* have been shown to influence its sensitivity to ethylene, a hormone that plays a critical role in the ripening process of tomato fruit [40]. Additionally, *MdbHLH3* has been identified as a promoter of fruit softening and an enhancer of ethylene release, thereby impacting the storability of apples [41]. The expression of *VvbHLH105* has unveiled a connection among oxidative signaling, transcriptional regulation, and the ripening process in grapes. This relationship was substantiated through EMSA and Y1H assays, which demonstrated that VvbHLH105 directly interacts with the G-box motif located in the promoter region of *VvHSP20-31* (Fig. 3F). Consequently, the expression of *VvbHLH105* is repressed by exogenous H_2O_2, leading to a diminished regulatory influence on the transcription of *VvHSP20-31*. This mechanism reflects the function of bHLH proteins in the stress response; however, it presents an avenue of research by establishing a connection between H_2O_2 signaling, transcriptional regulation, and the process of fruit ripening.

VvENO2 interacting with VvHSP20-31 and functions in the ripening process

Enolase plays a crucial role in the cellular energy metabolism of plants [51]. The ENO2 protein is encoded by the LOS2 (Low expression of osmotically responsive genes 2)/ENO2 locus [52]. In plants, three distinct isozymes of enolase have been identified: ENO1, ENO2, and ENO3. These isozymes demonstrate a significant level of conservation in their amino acid sequences (Fig. S6D and E). Within plant cells, glycolytic pathways operate autonomously in both the cytoplasm and the plastid. However, these two compartments

ACCEPTED MANUSCRIPT

Downloaded from academic.oup.com/hr/advance-article/doi/10.1093/hr/uhag485/9097232 by Bursa Uludag University user on 19 November 2026

can engage in interaction through specific transporter proteins located on the inner membrane of the plastid [53]. ENO2, a multifunctional protein that serves a significant functional role within the cytoplasm and nucleus, exhibits elevated expression levels throughout plant growth and development, with its expression being ten times greater than that of ENO1 and ENO3 [54, 55]. Our study identified an interaction between VvHSP20-31 and VvENO2, indicating that both proteins contribute comparably to the regulation of fruit ripening. While enolase is traditionally linked to glycolytic processes, its role in stress response and developmental mechanisms is becoming increasingly recognized [32, 52]. The inhibitory regulation of grape berry ripening genes by *VvENO2*, along with its physical interaction with VvHSP20-31, indicates that *VvENO2* is likely to play a significant role in the maintenance of ROS homeostasis. We propose that *VvENO2* may influence the availability of substrates for antioxidant pathways or may directly modulate *VvHSP20-31*, thereby augmenting its chaperone activity. This interaction elucidates the postponed berry ripening associated with the overexpression of *VvENO2*, potentially due to the redistribution of energy and a decrease in ROS, which may impede the signaling pathways related to ripening senescence. Subsequent research should investigate whether the enzymatic activity of *VvENO2* is critical for its regulatory role or if it functions solely as a scaffolding protein.

H_2O_2 acts as a vital signaling molecule in the process of fruit ripening

H_2O_2 classified as a reactive oxygen species, plays a crucial role in nearly all aspects of plant growth and development [56]. To ensure optimal growth, plants have evolved a series of mechanisms for the generation and scavenging of hydrogen peroxide, which help to regulate its concentration within a specific range [57]. Our research indicates that H_2O_2 serves as a crucial signaling molecule in the post-translational regulatory mechanisms. The observed reduction in interactions between VvHSP20-31 and VvENO2, as evidenced by BiFC and LCI assays, suggests that oxidative conditions destabilize the protein complex,

ACCEPTED MANUSCRIPT

Downloaded from academic.oup.com/hr/advance-article/doi/10.1093/hr/uhag485/9097232 by Bursa Uludag University user on 19 November 2026

thereby diminishing these interactions [58]. The expression levels of *VvbHLH105*, *VvHSP20-31*, and *VvENO2* were observed to exhibit a negative correlation with the endogenous H_2O_2 level, as evidenced by DAB staining of transgenic berry slices and leaves, along with the quantification of H_2O_2 content. In the transcriptomic analysis of early ripening grapes treated with 'Kyoho', a reduction in the expression levels of the *VvbHLH105, VvHSP20-31*, and *VvENO2* genes was noted. Furthermore, a transient *in vitro* transformation assay conducted on grape berries indicated that the endogenous H_2O_2 level in gene-silenced berries was elevated. These findings align with the results of our previous study [19]. In summary, our study contributes a mechanistic understanding by establishing a connection between H_2O_2 and transcriptional regulation as well as protein interactions. The dual functions of H_2O_2, serving both as a stress signal and as a developmental trigger, underscore its diverse roles in plant physiology; despite, the requirement to maintain tight cellular regulation of H_2O_2 to prevent oxidative damage [56].

Materials and methods

Plant materials and growth conditions

The grape variety 'Kyoho' was cultivated very healthy in the vineyard of Henan University of Science and Technology (HAUST) by performing all cultural practices thoroughly throughout the production season. Sterilized *Arabidopsis thaliana (L.)* seeds were planted on solid MS medium and kept at 4 °C for one day to meet their chilling requirement, which also helps their germination. Following this, the seeds were exposed to a photoperiod of 16 hours of light and 8 hours of darkness at a temperature of 25 °C. Once the second true leaves developed, the seedlings were transferred to nutrient-rich soil for further cultivation, with regular watering throughout the growth period.

The *Arabidopsis* plants were cultivated to reach a mossy state, at which point the stem tissues were excised. The plants were then cultivated for an additional period to ensure that

ACCEPTED MANUSCRIPT

Downloaded from academic.oup.com/hr/advance-article/doi/10.1093/hr/uhag485/9097232 by Bursa Uludag University user on 19 November 2026

all disks of *Arabidopsis* maintained a mossy appearance. Subsequently, the seed pods were removed, leaving only the flower buds in preparation for the transgenic infestation test.

Full Micro-Tom tomato seeds were chosen, subjected to sterilization, and subsequently sown in MS solid medium. The seeds underwent vernalization at 4 °C for one day, followed by a three-day dark incubation, after which they were exposed to light until germination and the development of cotyledons, preparing them for subsequent experimental procedures. *N. benthamiana* tobacco was cultivated at a temperature of 25 °C under a photoperiod of 16 hours of light and 8 hours of darkness. For the transient transformation assay, two to three leaves from four-week-old, healthy tobacco seedlings were utilized, with three biological replicates of the tobacco plants used in the study.

RNA, DNA extraction and quantitative real-time polymerase chain reaction (RT-qPCR) assay

Total RNA was isolated utilizing the RNA-prep pure polysaccharide polyphenol plant total RNA extraction kit (Tiangen, Beijing, China). Subsequently, a reverse transcription kit (Vazyme, Nanjing, China) was employed to convert the total RNA into cDNA. The relative expression levels of the grape *VvUbiquitin* gene (GenBank accession No: MH114011.1) were quantified using the $2^{-\Delta\Delta Ct}$ method. For all quantification experiments, three biological replicates were employed [59]. The resultant lines were characterized through RT-qPCR and DNA sequencing. Total DNA was extracted utilizing the FastPure Plant DNA Isolation Mini Kit-BOX 2 Genome Extraction Kit (Vazyme, Nanjing, China). The primers used in RT-qPCR are shown in Table S4.

3,3-Diaminobenzidine (DAB) staining and determination of H_2O_2 content

DAB staining was conducted utilizing a commercially available kit (Biotopped, Beijing, China). Transgenic grape berry sections, tomato leaves, and *Arabidopsis* seedlings were

ACCEPTED MANUSCRIPT

Downloaded from academic.oup.com/hr/advance-article/doi/10.1093/hr/uhag485/9097232 by Bursa Uludag University user on 19 November 2026

incubated in a 1 mg/ml DAB working staining solution at 37 °C overnight. Subsequently, the samples were stained using anhydrous ethanol for 30 minutes in a water bath maintained at 80 °C, after which photographs were taken for documentation purposes. The plant tissues were homogenised into a powder using liquid nitrogen, followed by the addition of a 10×PBS buffer at a volume nine times greater than the weight of the tissue, adhering to a weight-to-volume ratio of 1∶9 (g∶ml). The mixture was vortexed and agitated for one minute, subsequently subjected to centrifugation at 12,000 rpm for ten minutes. The supernatant was collected, and the concentration of H_2O_2 was quantified utilizing a hydrogen peroxide assay kit (Jiancheng, Nanjing, China).

Subcellular localization

The complete coding sequences (excluding stop codons) of the target genes (*VvbHLH105*, *VvHSP20-31*, *VvENO2*) were cloned into the *Eco*R I and *Bam*H I restriction sites of the vector 101LYFP for the purpose of recombination. Subsequently, the resulting recombinant vector, along with the empty plasmid, was introduced into the *Agrobacterium tumefaciens* strain GV3101 (Weidibio, Shanghai, China). For the purpose of transient expression, the bacterium was resuspended in a buffer solution. The injection solution was formulated based on the following ratio: YFP-gene/YFP empty∶Marker∶P19 helper plasmid = 4∶3∶3. This solution was subsequently injected into the abaxial surface of the leaves of *N. benthamiana* tobacco, which were approximately 4-6 weeks old. Following the injection, the plants were cultured for a duration of 2-3 days to facilitate the observation of YFP fluorescence, which was conducted using a laser confocal microscope (Olympus, FV3000). The primers used in subcellular localization are shown in Table S4.

GUS staining

The promoter sequences of the target genes (*VvbHLH105*, *VvHSP20-31*, *VvENO2*) were

ACCEPTED MANUSCRIPT

Downloaded from academic.oup.com/hr/advance-article/doi/10.1093/hr/uhag485/9097232 by Bursa Uludag University user on 19 November 2026

589 cloned and were ligated to pC0390-GUS fusion vectors. Subsequently, tobacco leaves were
590 subjected to transient transformation via vacuum infiltration. In this process, the infiltrated
591 tobacco leaves were positioned in trays, with their petioles moistened using sterile water.
592 Skimmed cotton was then applied, and the leaves were covered with plastic wrap. After a
593 24-hour incubation period, the leaves were treated with 300 mmol/L H_2O_2, 100 μmol/L
594 ABA, and 100 μmol/L IAA, with deionized ddH_2O serving as a control. Following an
595 additional 24 hours of incubation, the leaves were subjected to a GUS staining solution
596 (Cygnus, Nanjing, China). The samples were then placed in a constant-temperature
597 incubator set at 37 °C for overnight incubation. Subsequently, the leaves were incubated in
598 anhydrous ethanol, which had been heated to 37 °C, until complete decolourization was
599 achieved. The staining results were then observed and photographed. The primers used in
600 this assay are shown in Table S4.

601

602 Bimolecular fluorescence complementation assay (BiFC)

603 The fusion vectors nYFP-VvHSP20-31 and cYFP-VvENO2 were constructed by inserting
604 the coding sequences (CDS) of *VvHSP20-31* and *VvENO2*, respectively, into the nYFP and
605 cYFP vectors, omitting the stop codon. An *Agrobacterium* infiltration solution containing
606 both nYFP-VvHSP20-31 and cYFP-VvENO2 was co-injected into *Nicotiana benthamiana*
607 leaves in equal proportions, with nYFP-P1 and cYFP-P2 serving as a positive control, and
608 nYFP and cYFP as a negative control. Following a 1-day incubation period under low-light
609 conditions, the tobacco leaves were treated with a 300 mmol/L H_2O_2 solution. After 2 to 3
610 days, yellow fluorescent protein (YFP) signals, which were excited at 580 nm, were
611 detected using a laser confocal microscope (Olympus, FV3000) to assess the interaction
612 between VvHSP20-31 and VvENO2. The primers used in BiFC are shown in Table S4.

613

614 Split-luciferase assay (LCI)

ACCEPTED MANUSCRIPT

Downloaded from academic.oup.com/hr/advance-article/doi/10.1093/hr/uhag485/9097232 by Bursa Uludag University user on 19 November 2026

615 The coding sequences of the full-length *VvHSP20-31* and *VvENO2* were successfully
616 cloned into the pCAMBIA1300-nLUC and pCAMBIA1300-cLUC vectors, respectively,
617 leading to the development of VvHSP20-31-nLUC and VvENO2-cLUC fusion constructs.
618 Following this, *Agrobacterium tumefaciens* strains containing these plasmids were
619 employed to infiltrate tobacco leaves. After a 24-hour incubation period in low-light
620 conditions, the tobacco leaves were subjected to treatment with a 300 mmol/L H_2O_2
621 solution and subsequently incubated in low light for an additional 24 hours. Samples were
622 then collected from the infiltrated areas of the leaves to evaluate LUC activity. Following
623 the application of 1 mM D-luciferin potassium salt (Solarbio, Beijing, China) to the abaxial
624 surface of the leaves, fluorescence imaging was performed using a plant *vivo* imaging
625 system (PlantView) to capture the emitted fluorescence signal. The primers used in LCI
626 are shown in Table S4.
627

628 **Yeast two-hybrid library screening and Y2H assay**

629 The pGBKT7-*VvHSP20-31* was employed as a bait vector, which was subsequently
630 transformed into the AH109 strain. The library plasmid pGADT7 grape cDNA was then
631 introduced into this strain. Following transformation, the yeast cells were subjected to
632 amplification using the Yeast Positive Cloning Kit (Yeast Colony Rapid Detection Kit,
633 Ruiyuan, China). The resulting DNA was sequenced and analyzed through BLAST
634 comparison with sequences available in the GenBank database.

635 The CDS of *VvENO2* was incorporated into the Gal4 activation domain of the
636 pGADT7 vector, serving as a prey vector, utilizing gene-specific primers. Following the
637 identification of a concentration that effectively inhibited the self-activation of *VvHSP20-*
638 *31*, the recombinant vector was co-transformed into the Y2H Gold yeast strain (Weidibio,
639 Shanghai, China). Positive yeast colonies were subsequently selected on SD medium
640 deficient in two nutrients and on SD medium deficient in four nutrients. After an incubation
641 period of 3 to 5 days at 30 °C, the interaction between VvHSP20-31 and the VvENO2

ACCEPTED MANUSCRIPT

Downloaded from academic.oup.com/hr/advance-article/doi/10.1093/hr/uhag485/9097232 by Bursa Uludag University user on 19 November 2026

protein was assessed through the growth of the transgenic yeast cells and α-galactosidase staining. The primers used in Y2H are shown in Table S4.

GST Pull-down assay

GST fusion proteins were employed for the analysis of protein interactions. In the GST pull-down assay, the complete cDNA of *VvENO2* was cloned into the pET-28a vector, while the full-length cDNA of *VvHSP20-31* was incorporated into the pGEX-6p vector. The resultant recombinant proteins were utilized in the GST pull-down assay [60]. The interaction between VvHSP20-31 and VvENO2 was subsequently examined using SDS-PAGE and Western blotting techniques. The primers used in pull-down are shown in Table S4.

Yeast one-hybrid library screening and Y1H assay

The *VvHSP20-31* promoter fragment, measuring 559 base pairs, was amplified through polymerase chain reaction (PCR) and subsequently inserted into the *Kpn* I/*Xho* I sites of the pAbAi vector. This construct was linearized using the restriction enzyme *Bstb* I and transformed into the Y1H Gold yeast strain, where it served as bait in conjunction with a nuclear sub-library plasmid (Shanghai OE Biotech. Co., Ltd, China) utilized as prey. Individual colonies were isolated and subjected to PCR amplification for sequencing to identify the interacting transcription factors. A BLAST analysis of each candidate sequence was conducted utilizing the grape reference genome database (https://plants.ensembl.org/Vitis_vinifera/Info/Index).

Yeast one-hybrid (Y1H) was conducted by inserting the CDS of *VvbHLH105* into the pGADT7 vector, which served as the prey vector. Concurrently, promoter fragments of *VvHSP20-31* were incorporated into the pAbAi vector, functioning as the bait vector. The linearized recombinant plasmid pAbAi was subsequently transformed into the Y1H Gold

ACCEPTED MANUSCRIPT

Downloaded from academic.oup.com/hr/advance-article/doi/10.1093/hr/uhag485/9097232 by Bursa Uludag University user on 19 November 2026

strain (Weidibio, Shanghai, China). Following the identification of positive transformants, the pGADT7 recombinant plasmid was co-transfected into the prepared yeast strain. The transformed yeast was then plated on SD-Leu medium supplemented with an inhibitory concentration of AbA and incubated at 30 °C for a duration of 3-5 days. The growth of the yeast cells was subsequently monitored to assess the interaction between the VvbHLH105 and *VvHSP20-31* promoter. The primers used in Y1H are shown in Table S4.

Transient dual-luciferase reporter assay (DLR)

The CDS of *VvbHLH105* was incorporated into the pSAK277 vector to serve as an effector plasmid. Concurrently, the promoter fragment of *VvHSP20-31* was fused into the pGreenII-0800-LUC vector to function as a reporter plasmid. A mixed *Agrobacterium* infiltration solution, with a ratio of effector gene to reporter gene of 10∶1 (v∶v), was introduced into tobacco leaves. Following a 48-hour incubation period under low-light conditions, samples were collected from the infiltrated regions of the leaves. The activities of LUC and REN were subsequently assessed using a dual-luciferase reporter assay kit (Promega, Beijing, China). Additionally, the abaxial surface of the leaves was infiltrated with a 1 mM solution of D-luciferin potassium salt (Solarbio, Beijing, China), and the resulting fluorescein fluorescence signals were captured using a plant live imaging system (PlantView). The primers used in this assay are shown in Table S4.

Electrophoretic mobility shift assay (EMSA)

The CDS of *VvbHLH105* was inserted into the His-tagged pET-28a expression vector, facilitating the prokaryotic expression of the recombinant His-tagged VvbHLH105 protein. Biotin-labeled probes containing G-box elements, as well as their mutant counterparts within the *VvHSP20-31* promoter, were utilized, with unlabeled probes serving as binding competitors. An EMSA was conducted to analyze the interaction between the purified

ACCEPTED MANUSCRIPT

Downloaded from academic.oup.com/hr/advance-article/doi/10.1093/hr/uhag485/9097232 by Bursa Uludag University user on 19 November 2026

VvbHLH105 protein and the probes [61]. The specific primers and probes employed in this study are detailed in Table S4.

Transient transformation assay in grape berries

Utilizing cDNA from 'Kyoho' grapes as a template, the complete CDS of *VvbHLH105*, *VvHSP20-31*, and *VvENO2* were inserted into pIR vectors that had been enzymatically cleaved with *Bam*H I and *Xba* I, resulting in the construction of overexpression vectors: pIR-*VvbHLH105*-OE, pIR-*VvHSP20-31*-OE, and pIR-*VvENO2*-OE. Additionally, silencing vectors were developed, namely pIR-*VvbHLH105*-RNAi, pIR-*VvHSP20-31*-RNAi, and pIR-*VvENO2*-RNAi, by reverse ligating the full-length CDSs of *VvbHLH105*, *VvHSP20-31*, and *VvENO2* into the pIR vectors following *Bam*H I and *Xba* I digestion [62, 63]. Approximately 30 days post-flowering, an injection needle was inserted into the stem of 'Kyoho' grape clusters, followed by the insertion of a capillary tube into the punctured site. Subsequently, approximately 200 ng of DNA plasmid (50 μL) was introduced into the capillary tube until fully absorbed by the grape clusters. This injection procedure was repeated three times, with intervals of seven days between each application. The grape berries were harvested three days following the final treatment. One biological replicate includes three clusters. After treatment, the berries with similar directions and locations in different clusters were sampled from the clusters with uniform development, ensuring that the selected berries have consistent ripeness for subsequent analysis, then were subsequently stored at -80°C for physiological measurements and quantitative analysis. Data analysis was conducted utilizing GraphPad software. The primers used in this assay are shown in Table S4.

Tomato genetic transformation

The Micro-Tom tomato variety served as the experimental material for this study. The

ACCEPTED MANUSCRIPT

Downloaded from academic.oup.com/hr/advance-article/doi/10.1093/hr/uhag485/9097232 by Bursa Uludag University user on 19 November 2026

complete CDS of *VvHSP20-31* and *VvENO2* were inserted into the *Bam*H I-digested pCAMBIA2300 vector to create overexpression constructs, specifically pCAMBIA2300-*VvHSP20-31*-OE and pCAMBIA2300-*VvENO2*-OE. The transformation of tomato plants was conducted using *Agrobacterium* strain GV3101 (Weidibio, Shanghai, China) through the leaf infiltration method [64]. The plants were subjected to a selection process every 20 days until resistant shoots emerged. These shoots were subsequently transferred to a rooting medium, where they developed into fully formed plants. The plants were then transplanted to a greenhouse until transgenic plants exhibiting positive traits were obtained. Following this, phenotypic observations were conducted, and samples were collected for further experimental analyzes. Data analysis was conducted utilizing GraphPad software. The primers used in this assay are shown in Table S4.

Arabidopsis stabilising transformation

In the present study, we utilized Colombian wild-type (WT) *Arabidopsis* and developed overexpression vectors, specifically pCAMBIA2300-*VvHSP20-31*-OE and pCAMBIA2300-*VvENO2*-OE, by ligating the complete CDS of *VvHSP20-31* and *VvENO2* into the *BamH* I-digested pCAMBIA2300 vector. The transformation of *Arabidopsis* was conducted using the inflorescence infestation method [65]. *Arabidopsis* flower buds were subjected to a 10-minute immersion in centrifuge tubes containing an *Agrobacterium* infiltration solution. Following this infiltration period, any excess bacterial solution was removed using absorbent paper, and the buds were subsequently incubated in the dark for 24 hours. This was followed by a period s normal light culture until transgenic plants of the T3 generation were successfully obtained. The transgenic plants were then screened on MS medium supplemented with 50 μg/mL kanamycin. Positive transgenic plants were identified through genomic PCR utilizing specific primers as outlined in the literature [66, 67]. The primers used in this assay are shown in Table S4.

ACCEPTED MANUSCRIPT

Downloaded from academic.oup.com/hr/advance-article/doi/10.1093/hr/uhag485/9097232 by Bursa Uludag University user on 19 November 2026

Statistical analysis

All real-time PCR and other quantitative analyzes were conducted at least 3 times. One-way ANOVA is used to assess the variation in the dependent variable attributable to a single independent variable. Two-way ANOVA was employed to assess the differential effects of two independent variables on the dependent variable. For multiple comparisons, one-way and two-way ANOVA, followed by Tukey's multiple comparison tests, was used for significance analysis. The statistical analysis was performed using GraphPad Prism software (version 9.0) by entering the raw data.

Author contributions

D.L.G. planned and designed the research. J.L.X. performed the experiments, analyzed the data and wrote the manuscript draft, with the assistance of J.Q.X., K.Y.D., D.D.Z., S.J.L., S.P.C. J.G.L. and A.A. finalized revision of the manuscript. All authors have read and approved the final version of the manuscript.

Acknowledgements

This work was financially supported by National Natural Science Foundation of China, (NSFC: 32472662) and Natural Science Foundation of Henan (232300421112).

Conflicts of interest statement

The authors declare that they have no competing interests.

Data availability

All data generated or analyzed during this study are included in this published article and its Supplementary materials.

ACCEPTED MANUSCRIPT

Downloaded from academic.oup.com/hr/advance-article/doi/10.1093/hr/uhag485/9097232 by Bursa Uludag University user on 19 November 2026

Accession numbers

The data that support the findings of this study are available from the corresponding author upon reasonable request. Sequence data from this article can be found in the NCBI Database under the following accession numbers: *VvHSP20-31* (Vitvi13g02024); *VvENO2* (Vitvi08g01520); *VvbHLH105* (Vitvi19g00406); *VvAG2* (Accession No: TC62522); *VvADH2* (Vitvi04g01670); *VvMYBPA1* (Vitvi15g00938); *VvMSA* (Vitvi18g02973); *VvHT* (Accession No: RB004G11); *VvSEP3* (Vitvi01g01677); *VvCTG* (Vitvi15g00643); *VvGRIP4* (Vitvi05g01931).

Supplementary material

Supplementary material is available at Horticulture Research online.

References

1. Motta S, Cassino C, Bosso A. *et al.* Characterization of 37 enological tannins using a multiple technique approach: Linear sweep voltammetry as a rapid method both for classification and determination of antioxidant properties. *Food Chem.* 2025;463:141475.
2. Seymour GB, Østergaard L, Chapman NH. *et al.* Fruit development and ripening. Annu. Rev. *Plant Biol.* 2013;64:219–41.
3. Guo SH, Zhang M, Feng MX. *et al.* miR156b-targeted *VvSBP8/13* functions downstream of the abscisic acid signal to regulate anthocyanins biosynthesis in grapevine fruit under drought. *Hortic. Res.* 2024;11:293.
4. Li ZQ, Chen CY, Zou DF. *et al.* Ethylene accelerates grape ripening via increasing *VvERF75*-induced ethylene synthesis and chlorophyll degradation. *Fruit Res.* 2023;3:1–9.
5. Arro J, Yang YZ, Song GQ. *et al.* Transcriptome analysis unveils a potential novel role of *VvAP1* in regulating the developmental fate of primordia in grapevine. *Fruit Res.* 2024;4:11.
6. Guo DL, Xi FF, Yu YH. *et al.* Comparative RNA-Seq profiling of berry development between table grape ‘Kyoho’ and its early-ripening mutant ‘Fengzao’. *BMC Genomics.* 2016;17:795.
7. Yu JQ, Yang XK, Gao HS. *et al.* Transcriptome atlas provides novel insights into ABA-mediated modulation of strawberry fruit ripening and quality. *Hortic. Adv.* 2025;3:16.

ACCEPTED MANUSCRIPT

Downloaded from academic.oup.com/hr/advance-article/doi/10.1093/hr/uhag485/9097232 by Bursa Uludag University user on 19 November 2026

8. Zuo DD, Yang L, Li RY. *et al.* Histone H3K4 demethyltransferase VvJMJ14 promotes H_2O_2 inducing fruit ripening in grape. *Plant J.* 2025;124:70642.
9. Atak A, Akgün M, Şen A. *et al.* Evaluation of Quality Characteristics and Cultivar Candidate Potentials of Hybrid Genotypes Obtained from Different *Vitis* Species. *Horticulturae.* 2025;11:354.
10. Guo LL, Xi FF, Yu YH. *et al.* Studies of the riboflavin treatment for promoting the early ripening of 'Kyoho' grape berry. *Acta Hortic. Sin.* 2017;44:1861–70.
11. Wei TL, Wan YT, Liu HN. *et al.* CHH hypermethylation contributes to the early ripening of grapes revealed by DNA methylome landscape of 'Kyoho' and its bud mutant. *Hortic. Res.* 2025;12:285.
12. Huan C, Jiang L, An XJ. *et al.* Potential role of reactive oxygen species and antioxidant genes in the regulation of peach fruit development and ripening. *Plant Physiol. Biochem.* 2016;104:294–303.
13. Shen L, Ruan Y, Liu K. *et al.* Metabolism of reactive oxygen dynamic changes during tomato fruit ripening and senescence. *Acta Hortic*. 2008;768:517–23.
14. Kan J, Wang HM, Jin CH. *et al.* Changes of Reactive Oxygen Species and Related Enzymes in Mitochondria Respiratory Metabolism During the Ripening of Peach Fruit. *Agric. Sci. China.* 2010;9:138–146.
15. Quan LJ, Zhang B, Shi WW. *et al.* Hydrogen peroxide in plants: a versatile molecule of the reactive oxygen species network. *J. Integr. Plant Biol.* 2008;50:2–18.
16. Jimenez A, Creissen G, Kular B. *et al.* Changes in oxidative processes and components of the antioxidant system during tomato fruit ripening. *Planta.* 2002;214:751–8.
17. Pilati S, Brazzale D, Guella G. *et al.* The onset of grapevine berry ripening is characterized by ROS accumulation and lipoxygenase-mediated membrane peroxidation in the skin. *BMC Plant Biol.* 2014;14:87.
18. Chiriboga M-A, Bordonaba JG, Schotsmans WC. *et al.* Antioxidant potential of 'Conference' pears during cold storage and shelf life in response to 1-methylcyclopropene. *LWT - Food Sci. Technol.* 2013;51:170–6.
19. Guo DL, Wang ZG, Li Q. *et al.* Hydrogen peroxide treatment promotes early ripening of 'Kyoho' grape. *Aust. J. Grape Wine Res.* 2019;25:357–62.
20. Ji XR, Yu YH, Ni PY. *et al.* Genome-wide identification of small heat-shock protein (HSP20) gene family in grape and expression profile during berry development. *BMC Plant Biol.* 2019;19:433.
21. Waters ER, Vierling E. Plant small heat shock proteins-evolutionary and functional diversity. *New Phytol.* 2020;227:24–37.
22. Zhao P, Wang DD, Wang RQ. *et al.* Genome-wide analysis of the potato Hsp20 gene family: identification, genomic organization and expression profiles in response to heat stress. *BMC Genomics.* 2018;19:61.
23. Sewelam N, Kazan K, Hüdig M. *et al.* The *AtHSP17.4C1* Gene Expression Is Mediated by Diverse Signals that Link Biotic and Abiotic Stress Factors with ROS and Can Be a Useful Molecular Marker for Oxidative Stress. *Int. J. Mol. Sci.* 2019;20:3201.

ACCEPTED MANUSCRIPT

Downloaded from academic.oup.com/hr/advance-article/doi/10.1093/hr/uhag485/9097232 by Bursa Uludag University user on 19 November 2026

24. Sewelam N, Jaspert N, Van Der Kelen K. *et al.* Spatial H_2O_2 signaling specificity: H_2O_2 from chloroplasts and peroxisomes modulates the plant transcriptome differentially. *Mol. Plant.* 2014;7:1191–210.
25. Upadhyay RK, Tucker ML, Mattoo AK. Ethylene and *RIPENING INHIBITOR* Modulate Expression of *SlHSP17.7A, B* Class I Small Heat Shock Protein Genes During Tomato Fruit Ripening. *Front. Plant Sci.* 2020;11:975.
26. Jung YJ, Nou IS, Kang KK. Overexpression of Oshsp16.9 gene encoding small heat shock protein enhances tolerance to abiotic stresses in rice. *Plant Breed. Biotechnol.* 2014;2:370–9.
27. Zhang J, Chen H, Wang H. *et al.* Constitutive Expression of a Tomato Small Heat Shock Protein Gene *LeHSP21* Improves Tolerance to High-Temperature Stress by Enhancing Antioxidation Capacity in Tobacco. *Plant Mol. Biol. Rep.* 2016;34:399–409.
28. Xue M, You YW, Zhang LY. *et al.* ZmHsp18 screened from the ZmHsp20 gene family confers thermotolerance in maize. *BMC Plant Biol.* 2024;24:1048.
29. Port M, Tripp J, Zielinski D. *et al.* Role of Hsp17.4-CII as coregulator and cytoplasmic retention factor of tomato heat stress transcription factor HsfA2. *Plant Physiol.* 2004;135:1457–70.
30. Netasharir I, Isaacson T, Lurie S. *et al.* Dual role for tomato heat shock protein 21: protecting photosystem II from oxidative stress and promoting color changes during fruit maturation. *Plant Cell.* 2005;17:1829–38.
31. Eremina M, Rozhon W, Yang S. *et al.* ENO2 activity is required for the development and reproductive success of plants, and is feedback-repressed by AtMBP-1. *Plant J.* 2015;81:895–906.
32. Nahas Z, Ticchiarelli F, van Rongen M. *et al.* The activation of Arabidopsis axillary buds involves a switch from slow to rapid committed outgrowth regulated by auxin and strigolactone. *New Phytol.* 2024;242:1084–97.
33. Liu WC, Song RF, Qiu YM. *et al.* Sulfenylation of ENOLASE2 facilitates H_2O_2-conferred freezing tolerance in Arabidopsis. *Dev. Cell.* 2022;57:1883–98.
34. Yuste-Lisbona FJ, Fernández-Lozano A, Pineda B. *et al. ENO* regulates tomato fruit size through the floral meristem development network. *Proc. Natl. Acad. Sci. U. S. A.* 2020;117:8187–95.
35. Huang YY, Xing XJ, Jin JY. *et al.* CmbHLH110, a novel bHLH transcription factor, accelerates flowering in chrysanthemum. *Horticultural Plant J.* 2024;10:1437–48.
36. Li XX, Duan XP, Jiang HX. *et al.* Genome-wide analysis of basic/helix-loop-helix transcription factor family in rice and Arabidopsis. *Plant Physiol.* 2006;141:1167–84.
37. Xiao LN, Da QF. The Roles of BLH Transcription Factors in Plant Development and Environmental Response. Int. J. Mol. Sci. 2022;23:3731.
38. Gan ZY, Zhang YP, Yang CN. *et al.* A kiwifruit bHLH149 transcription factor modulates carotenoid biosynthesis by directly activating *LCYB* during postharvest ripening. *Fruit Res.* 2025;5:e003.

ACCEPTED MANUSCRIPT

Downloaded from academic.oup.com/hr/advance-article/doi/10.1093/hr/uhag485/9097232 by Bursa Uludag University user on 19 November 2026

886 39. Wu CJ, Cai DL, Li J. *et al.* Banana MabHLH28 positively regulates the expression of
887 softening-related genes to mediate fruit ripening independently or via cooperating
888 with MaWRKY49/111. *Hortic. Res.* 2024;11:53.
889 40. Zhang LC, Kang J, Xie QL. *et al.* The basic helix-loop-helix transcription factor
890 bHLH95 affects fruit ripening and multiple metabolisms in tomato. *J. Exp. Bot.*
891 2020;71:6311–27.
892 41. Wang WY, Yu JQ, Du MC. *et al.* Basic helix-loop-helix (bHLH) transcription factor
893 MdbHLH3 negatively affects the storage performance of postharvest apple fruit.
894 *Hortic. Plant J.* 2022;8:700–12.
895 42. Passaia G, Margis-Pinheiro M, Fialho FB. *et al.* Characterization of an early berry
896 development grape somatic variant (*Vitis labrusca* L. cv. Isabel Precoce). *Am. J. Plant*
897 *Sci.* 2014;5:3848–65.
898 43. Toledo-Ortiz G, Huq E, Quail PH. The Arabidopsis basic/helix-loop-helix transcription
899 factor family. *Plant Cell*. 2003;15:1749–70.
900 44. Ahmad A, Niwa Y, Goto S. *et al*. bHLH106 integrates functions of multiple genes
901 through their G-box to confer salt tolerance on *Arabidopsis*. *PLoS ONE*.
902 2015;10:e0126872.
903 45. Timperio AM, Egidi MG, Zolla L. Proteomics applied on plant abiotic stresses: role of
904 heat shock proteins (HSP). *J. Proteomics.* 2008;71:391–411.
905 46. Siddique M, Gernhard S, von Koskull-Döring P. *et al.* The plant sHSP superfamily:
906 five new members in Arabidopsis thaliana with unexpected properties. *Cell Stress*
907 *Chaperones*. 2008;13:183–97.
908 47. Liu WC, Zhao XM, Bai B. *et al.* RNA interference-induced silencing of the *SlHSP17.7*
909 gene delays fruit ripening in tomato. *J. Plant Biochem. Biotechnol.* 2022;32:153–62.
910 48. Wei ZL, Cheng YL, Zhou CC. et al. Genome-Wide Identification of Direct Targets of
911 the TTG1-bHLH-MYB Complex in Regulating Trichome Formation and Flavonoid
912 Accumulation in *Arabidopsis Thaliana*. Int. J. Mol. Sci. 2019;20:5014.
913 49. Qian YC, Zhang TY, Yu Y. *et al.* Regulatory Mechanisms of bHLH Transcription
914 Factors in Plant Adaptive Responses to Various Abiotic Stresses. *Front. Plant Sci.*
915 2021;12:677611.
916 50. Lim SH, Kim DH, Lee JY. R2R3- MYB repressor, BrMYB32, regulates anthocyanin
917 biosynthesis in Chinese cabbage. *Physiol. Plant.* 2024;176:14591.
918 51. Subramanian A, Miller DM. Structural analysis of alpha-enolase. Mapping the
919 functional domains involved in down-regulation of the c-myc protooncogene. *J. Biol.*
920 *Chem.* 2000;275:5958–65.
921 52. Lee H, Guo Y, Ohta M. *et al.* LOS2, a genetic locus required for cold-responsive gene
922 transcription encodes a bi-functional ENOLASE. *EMBO J.* 2002;21:2692–702.
923 53. Weber AP, Schwacke R, Flügge UI. Solute transporters of the plastid envelope
924 membrane. *Annu. Rev. Plant Biol.* 2005;56:133–64.
925 54. Andriotis VM, Kruger NJ, Pike MJ. *et al.* Plastidial glycolysis in developing
926 *Arabidopsis* embryos. *New Phytol.* 2010;185:649–62.

ACCEPTED MANUSCRIPT

Downloaded from academic.oup.com/hr/advance-article/doi/10.1093/hr/uhag485/9097232 by Bursa Uludag University user on 19 November 2026

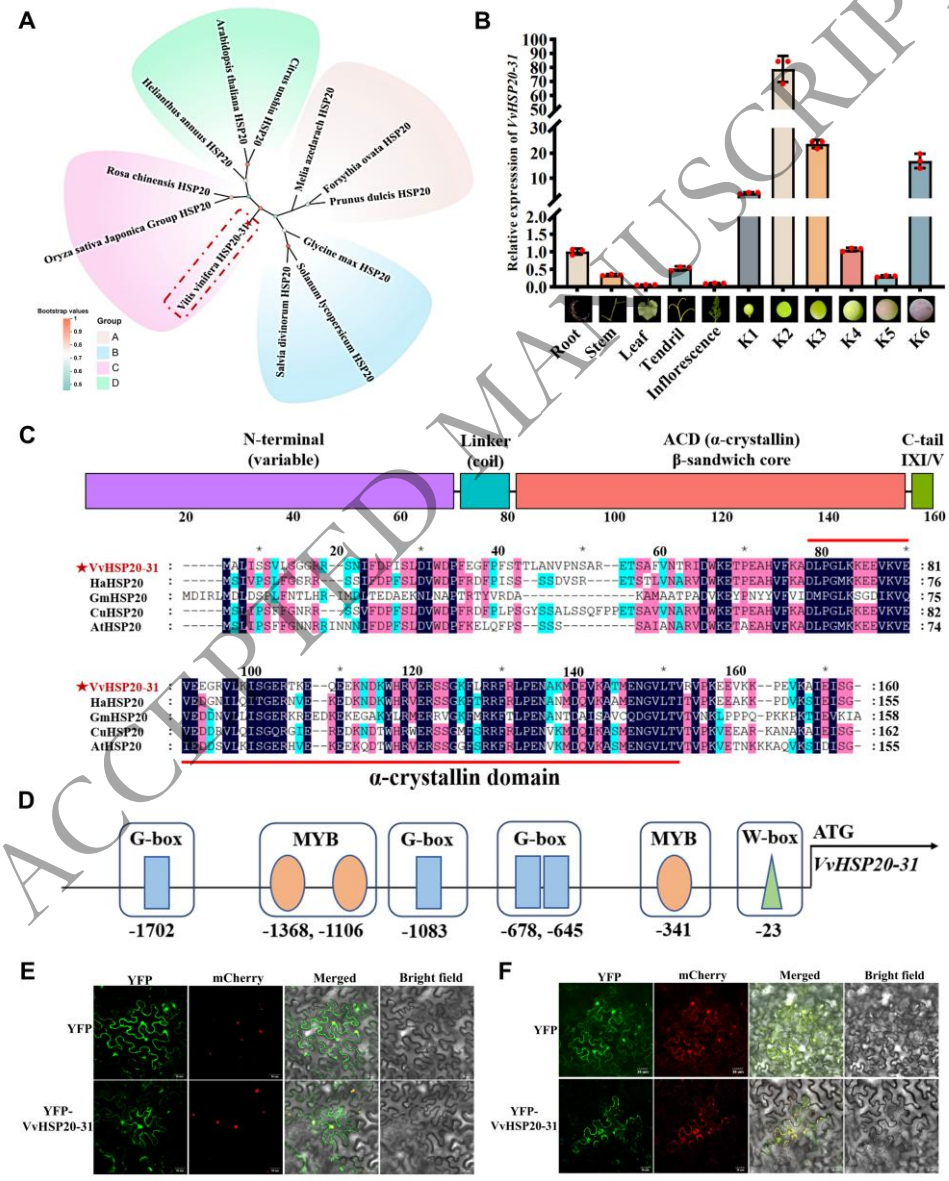
55. Liu Z, Zheng L, Pu L. *et al.* ENO2 Affects the Seed Size and Weight by Adjusting Cytokinin Content and Forming ENO2-bZIP75 Complex in *Arabidopsis thaliana*. *Front. Plant Sci*. 2020;11:574316.
56. Mittler R, Zandalinas SI, Fichman Y. *et al.* Reactive oxygen species signalling in plant stress responses. *Nat. Rev. Mol. Cell Biol.* 2022;23:663–79.
57. Apel K, Hirt H. Reactive oxygen species: metabolism, oxidative stress, and signal transduction. *Annu. Rev. Plant Biol.* 2004;55:373–99.
58. Rudan Dimlić M, Raić S, Močibob M. *et al.* Oxidative protein damage negatively affects protein-protein interaction: The case of KRAS-cRAF. *Biochem. Biophys. Res. Commun.* 2024;734:150792.
59. Livak KJ, Schmittgen TD. Analysis of relative gene expression data using real-time quantitative PCR and the 2(-Delta Delta C(T)) method. *Methods.* 2001;25:402–8.
60. Oh E, Zhu JY, Wang ZY. Interaction between BZR1 and PIF4 integrates brassinosteroid and environmental responses. *Nat. Cell Biol.* 2012;14(8):802-9.
61. Luan YT, Tang YH, Wang X. *et al.* Tree Peony R2R3-MYB Transcription Factor PsMYB30 Promotes Petal Blotch Formation by Activating the Transcription of the Anthocyanin Synthase Gene. *Plant Cell Physiol.* 2022;63:1101–16.
62. Peretz Y, Mozes-Koch R, Akad F. *et al.* A universal expression/silencing vector in plants. *Plant Physiol.* 2007;145: 1251-63
63. Jia HF, Zuo QQ, Sadeghnezhad E. *et al.* HDAC19 recruits ERF4 to the MYB5a promoter and diminishes anthocyanin accumulation during grape ripening. *Plant J.* 2023;113:127–44.
64. Chetty VJ, Ceballos N, Garcia D. *et al.* Evaluation of four Agrobacterium tumefaciens strains for the genetic transformation of tomato (Solanum lycopersicum L.) cultivar Micro-Tom. *Plant Cell Rep.* 2013;32:239–47.
65. Bent A. Arabidopsis thaliana floral dip transformation method. *Methods Mol. Biol.* 2006;343:87–103.
66. Fu XZ, Khan EU, Hu SS. *et al.* Overexpression of the betaine aldehyde dehydrogenase gene from Atriplex hortensis enhances salt tolerance in the transgenic trifoliate orange (*Poncirus trifoliata* L. Raf.). *Environ. Exp. Bot.* 2011;74:106–13.
67. Huang XS, Wang W, Zhang Q. *et al.* A basic helix-loop-helix transcription factor, PtrbHLH, of Poncirus trifoliata confers cold tolerance and modulates peroxidase-mediated scavenging of hydrogen peroxide. *Plant Physiol.* 2013;162:1178–94.

ACCEPTED MANUSCRIPT

Downloaded from academic.oup.com/hr/advance-article/doi/10.1093/hr/uhag485/9097232 by Bursa Uludag University user on 19 November 2026

Figure Legends

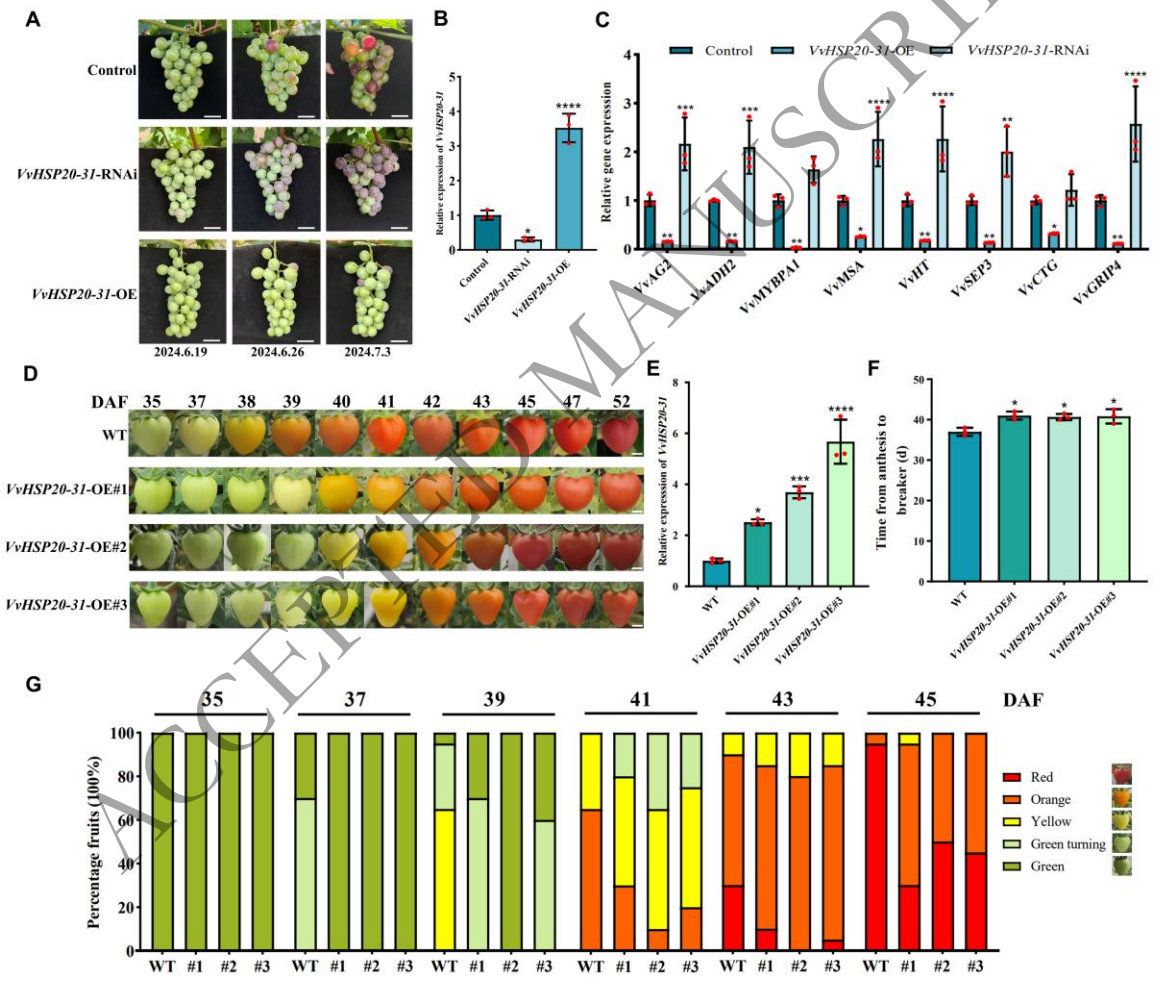
Figure 1 Identification and sequence analysis of *VvHSP20-31*. **(A)** Phylogenetic tree of *VvHSP20-31* with other species of HSP20. **(B)** Tissue-specific expression analysis of *VvHSP20-31*. Data are expressed as mean ± SD (n=3). **(C)** Amino acid sequence comparison and structural domains analysis of HSP20 across different species. *Helianthus annuus* HSP20 (KAF5821616.1), *Glycine max* HSP20 (NP_001346002.1), *Citrus unshiu* HSP20 (GAY37961.1), *Arabidopsis thaliana* HSP20 (AAD39328.1). **(D)** Schematic diagram of the *VvHSP20-31* promoter. The numbers indicate the distance from the start codon. **(E)** and **(F)** Subcellular localization of VvHSP20-31 in *N. benthamiana* leaves. The mCherry were used as nuclear and cytoplasmic localization markers, respectively. Scale bar, 30 μm.



ACCEPTED MANUSCRIPT

Downloaded from academic.oup.com/hr/advance-article/doi/10.1093/hr/uhag485/9097232 by Bursa Uludag University user on 19 November 2026

Figure 2 *VvHSP20-31* negatively regulates fruit ripening. **(A)** Transient overexpression or silencing of *VvHSP20-31* in grape berry phenotypes. pIR empty as control, scale bar is 1 cm. **(B)** RT-qPCR to detect the relative expression of *VvHSP20-31* in grape berry. **(C)** RT-qPCR for expression of grape ripening-related genes. **(D)** Tomato fruit phenotypes overexpressing *VvHSP20-31*, the WT used as a control, the scale bar is 0.5 cm. **(E)** RT-qPCR assay for relative expression of the *VvHSP20-31* in tomato fruits. **(F)** Number of days from anthesis to color transition in tomato fruits overexpressing *VvHSP20-31*. **(G)** Percentage of fruit of each color stage for each line of tomato on the same day. Data are expressed as mean ± SD (n=3), the figures of (**B**), (**E**) and (**F**) were analyzed by one-way ANOVA, the figure of (**C**) was analyzed by two-way ANOVA, there were significant differences between the treatment group and the control group (*0.01<*P*<0.05, 0.001<**P*<0.01, 0.0001<***P*<0.001, ****P*<0.0001).



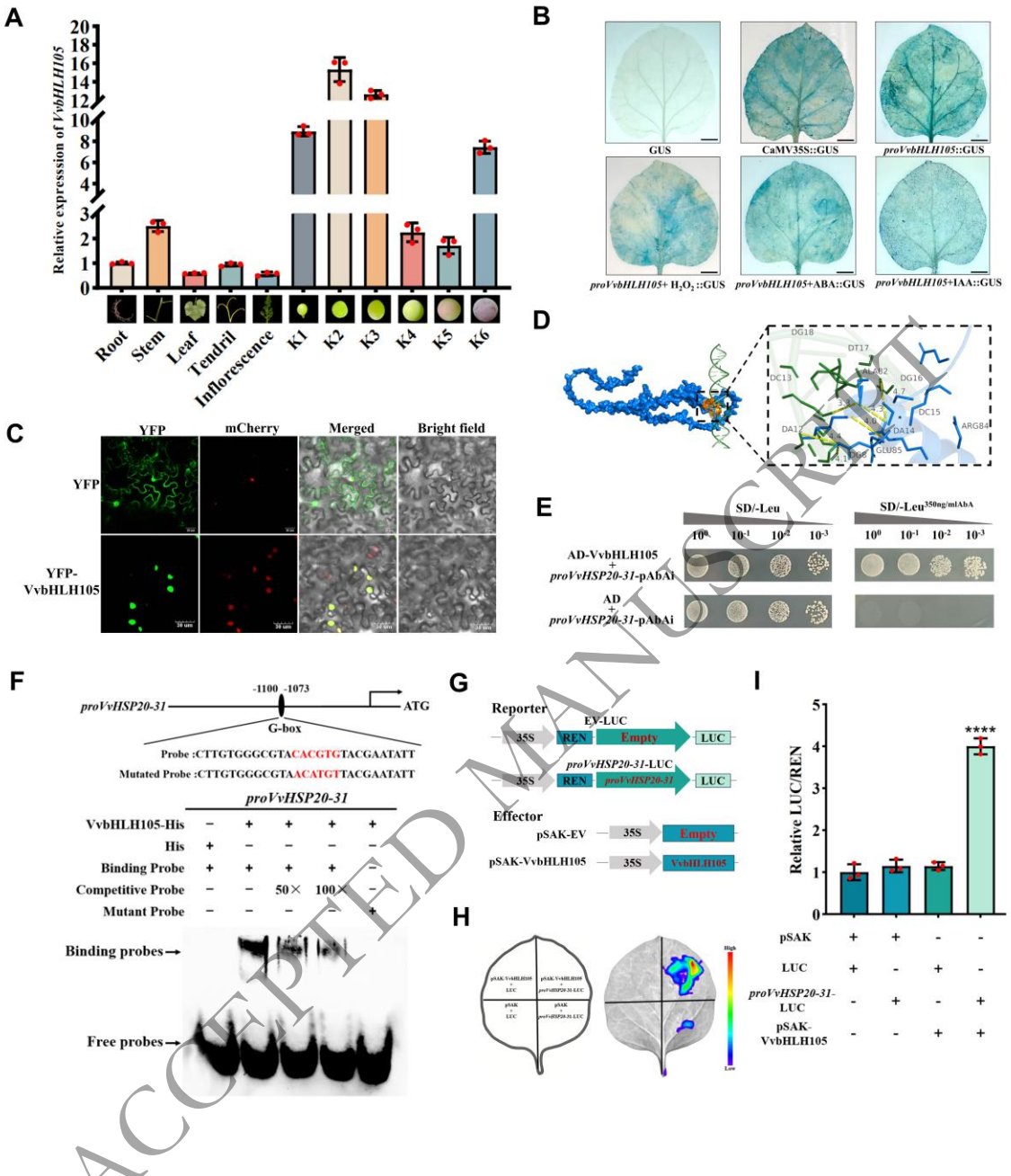
ACCEPTED MANUSCRIPT

Downloaded from academic.oup.com/hr/advance-article/doi/10.1093/hr/uhag485/9097232 by Bursa Uludag University user on 19 November 2026

Figure 3 Screening and characterization of VvbHLH105 and its binding to the *VvHSP20-31* promoter. **(A)** Tissue-specific expression analysis of *VvbHLH105*. Data are expressed as mean ± SD (n=3). **(B)** The assessment of the promoter activity of *VvbHLH105*. Utilizing GUS empty as a negative control and CaMV35S::GUS as a positive control, while *proVvbHLH105*::GUS was subjected to treatments with 300 mmol/L H_2O_2, 100 μmol/L ABA and IAA. Scale bar is 1 cm. **(C)** Subcellular localization of VvbHLH105. The mCherry was used as a nuclear localization marker. Scale bar, 30 μm. **(D)** AlphaFold3 predicts the binding between the *VvHSP20-31* promoter and the VvbHLH105 protein. The green DNA sequence is the *VvHSP20-31* promoter, and the blue protein is VvbHLH105. **(E)** Y1H analysis shows that VvbHLH105 binds to the *VvHSP20-31* promoter fragment. Yeast cells were cotransformed with prey AD-VvbHLH105 and bait constructed from the *proVvHSP20-31*-pAbAi fragment on SD/-Leu and SD/-Leu selective medium containing 350 ng/mL AbA. **(F)** EMSA showing that the VvbHLH105 protein binds directly to the *VvHSP20-31* promoter. Competing probes were added 50× and 100× times to lanes 3 and 4, and the binding probe CACGTG was replaced by ACATGT with the mutant probe ACATGT in lane 5. **(G)** Schematic diagram of the vectors for the dual-luciferase assay. **(H)** VvbHLH105 activates the expression of the *VvHSP20-31* promoter. **(I)** Relative LUC activity assay demonstrating that VvbHLH105 regulates the expression of the *VvHSP20-31* promoter. Data are expressed as mean ± SD (n=3). The figure of (**I**) was analyzed by one-way ANOVA, there were significant differences between the treatment group and the control group (*0.01<*P*<0.05, 0.001<**P*<0.01, 0.0001<***P*<0.001, ****P*<0.0001).

ACCEPTED MANUSCRIPT

Downloaded from academic.oup.com/hr/advance-article/doi/10.1093/hr/uhag485/9097232 by Bursa Uludag University user on 19 November 2026

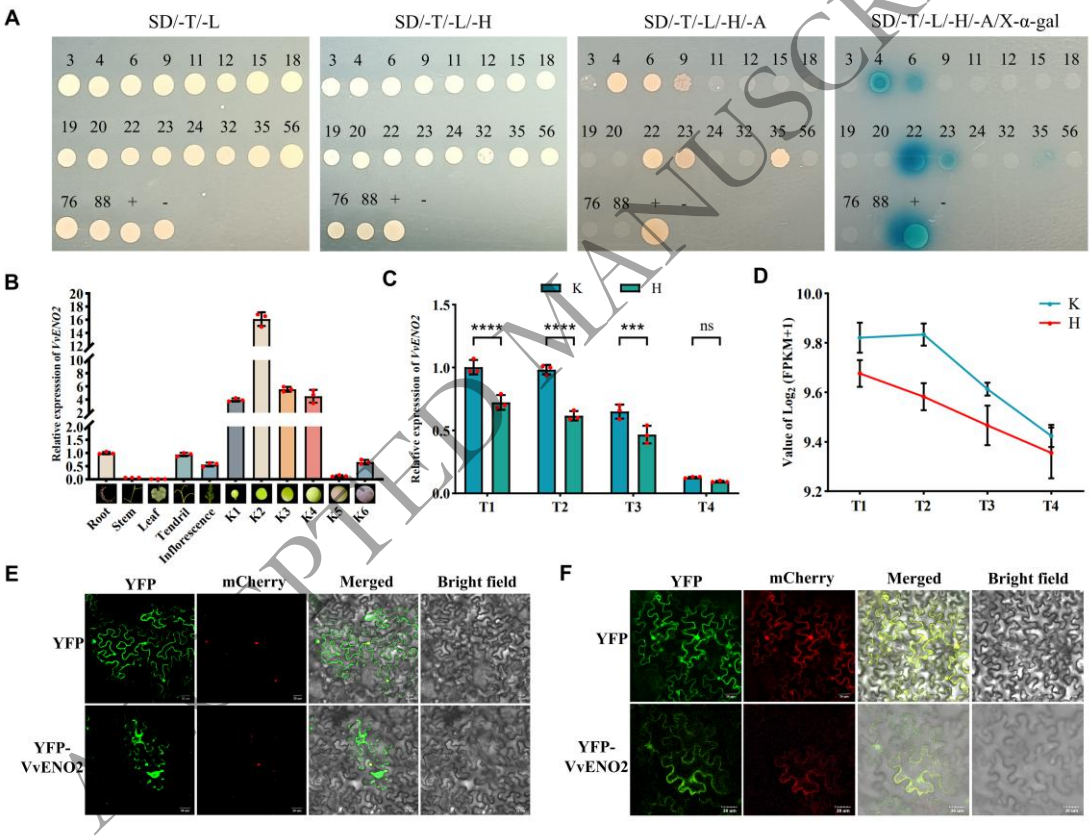


1006
1007

ACCEPTED MANUSCRIPT

Downloaded from academic.oup.com/hr/advance-article/doi/10.1093/hr/uhag485/9097232 by Bursa Uludag University user on 19 November 2026

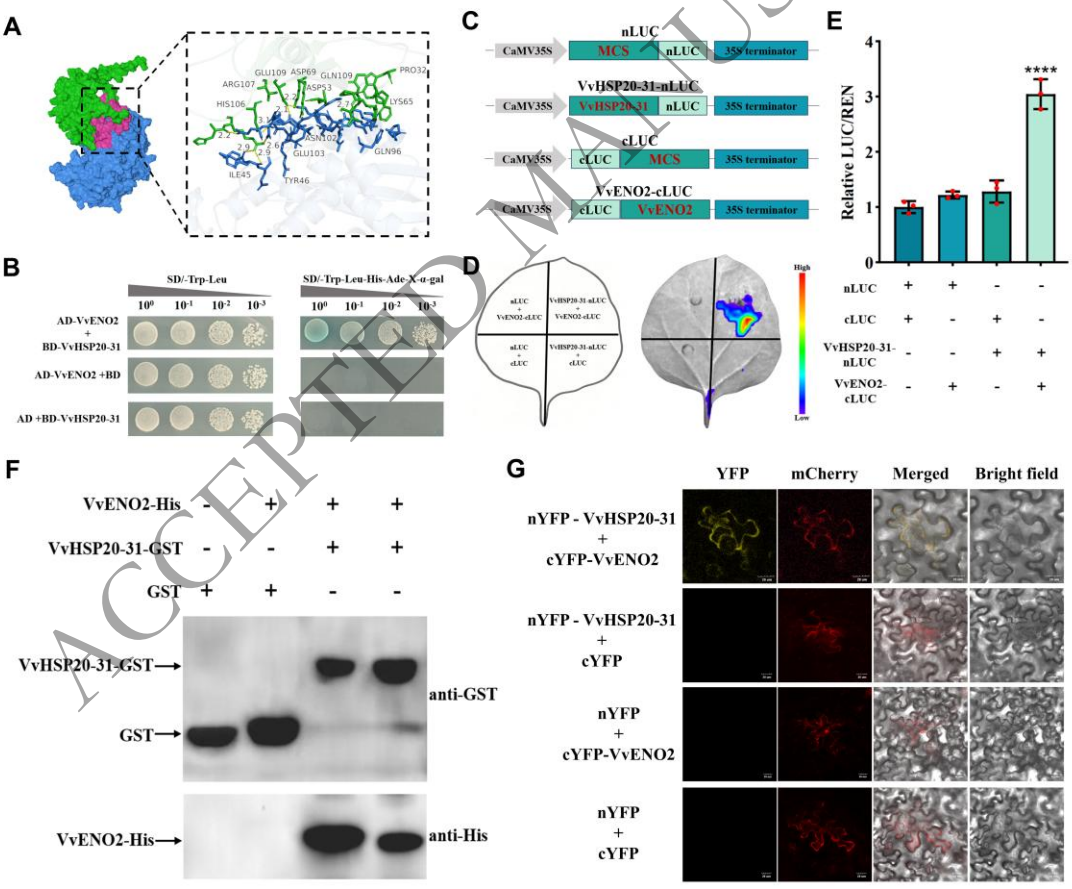
Figure 4 Screening, characterization, and expression analysis of *VvENO2*. **(A)** Validation of the yeast two-hybrid screen library. **(B)** Tissue-specific expression analysis of *VvENO2*. Data are expressed as mean ± SD (n=3). **(C)** RT-qPCR assay for relative expression of the *VvENO2* following H_2O_2 treatment. Samples were initially taken at 35 days after flowering (DAF) and continued at 10-day intervals until treated berry reached ripening, resulting in four sampling time points designated as T1 through T4. H for H_2O_2-treated berries, K for untreated control berries. Data are expressed as mean ± SD (n=3). **(D)** Relative expression of *VvENO2* in H_2O_2 treatment RNA-seq data. Samples were initially taken at 35 days after flowering (DAF) and continued at 10-day intervals until treated berry reached ripening. H for H_2O_2-treated berries, K for untreated control berries. **(E)** and **(F)** Subcellular localization of VvENO2. The mCherry were used as nuclear and cytoplasmic localization markers, respectively. Scale bar, 30 μm.



ACCEPTED MANUSCRIPT

Downloaded from academic.oup.com/hr/advance-article/doi/10.1093/hr/uhag485/9097232 by Bursa Uludag University user on 19 November 2026

Figure 5 VvENO2 interacts with the VvHSP20-31. **(A)** Prediction of VvHSP20-31 and VvENO2 protein interactions using AlphaFold3 and PyMOL for visualization. Green proteins are VvHSP20-31 and blue proteins are VvENO2. **(B)** Y2H analysis showed that VvHSP20-31 interacted with the VvENO2 protein. AD-VvENO2+BD and AD+BD-VvHSP20-31 were used as negative controls. **(C)** Schematic diagram of the vectors for the luciferase complementation assay. **(D)** Live imaging revealed that VvHSP20-31 interacts with VvENO2. **(E)** Relative LUC activity revealed that VvHSP20-31 interacts with VvENO2. **(F)** GST pull-down assay between VvHSP20-31 and VvENO2.The proteins VvHSP20-31-GST and VvENO2-His (VvENO2+VvHSP20-31) in lane 4, and GST empty tag and VvENO2-His (GST+VvENO2) in lane 2, were incubated separately. After elution with GSH eluent, they were detected by Western blot. **(G)** BiFC analysis reveals the interaction between VvHSP20-31 and VvENO2. The leaves of *N. benthamiana* tobacco were infested with nYFP-VvHSP20-31+cYFP-VvENO2 as the validation group, and nYFP+cYFP, nYFP-VvHSP20-31+cYFP, and nYFP+cYFP-VvENO2 as the negative control and were detected under a laser confocal microscope yellow fluorescent protein (YFP) signal. The mCherry was used as cytoplasmic localization marker. Scale bar, 20 μm.



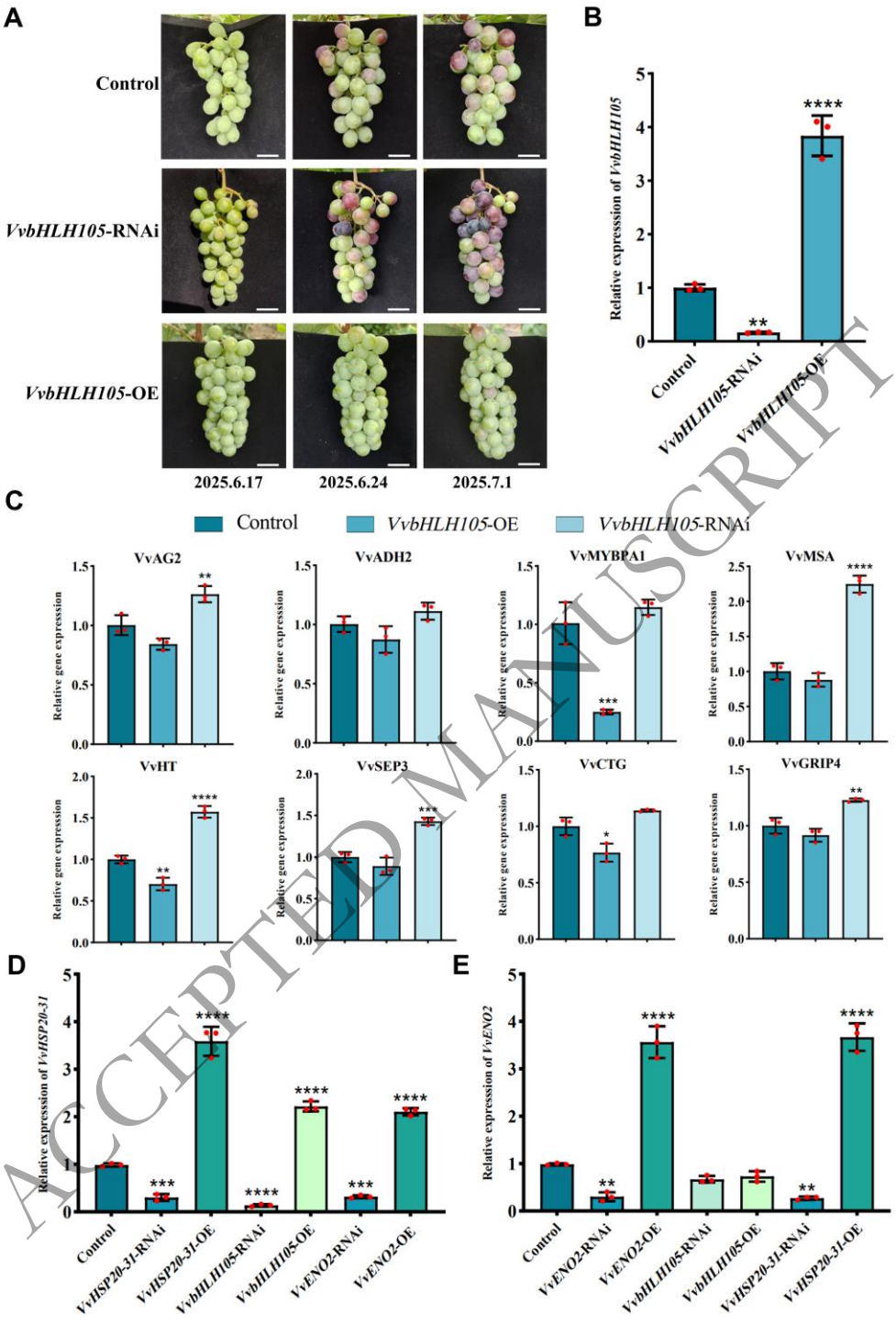
ACCEPTED MANUSCRIPT

Downloaded from academic.oup.com/hr/advance-article/doi/10.1093/hr/uhag485/9097232 by Bursa Uludag University user on 19 November 2026

Figure 6 *VvbHLH105* negatively regulates grape berry ripening. **(A)** Transient overexpression or silencing of *VvbHLH105* in grape berry phenotypes. The pIR empty was used as a control, and the scale bar was 1 cm. **(B)** RT-qPCR to detect the relative expression of *VvbHLH105*. **(C)** RT-qPCR to detect the expression of genes related to grape berry ripening. **(D)** Analysis of the relative expression of the *VvHSP20-31*. **(E)** Analysis of the relative expression of the *VvENO2*. The pIR empty was used as a control. Data are expressed as mean ± SD (n=3), the figures of (**B**), (**C**), (**D**) and (**E**) were analyzed by one-way ANOVA, there were significant differences between the treatment group and the control group (*0.01<*P*<0.05, 0.001<**P*<0.01, 0.0001<***P*<0.001, ****P*<0.0001).

ACCEPTED MANUSCRIPT

Downloaded from academic.oup.com/hr/advance-article/doi/10.1093/hr/uhag485/9097232 by Bursa Uludag University user on 19 November 2026

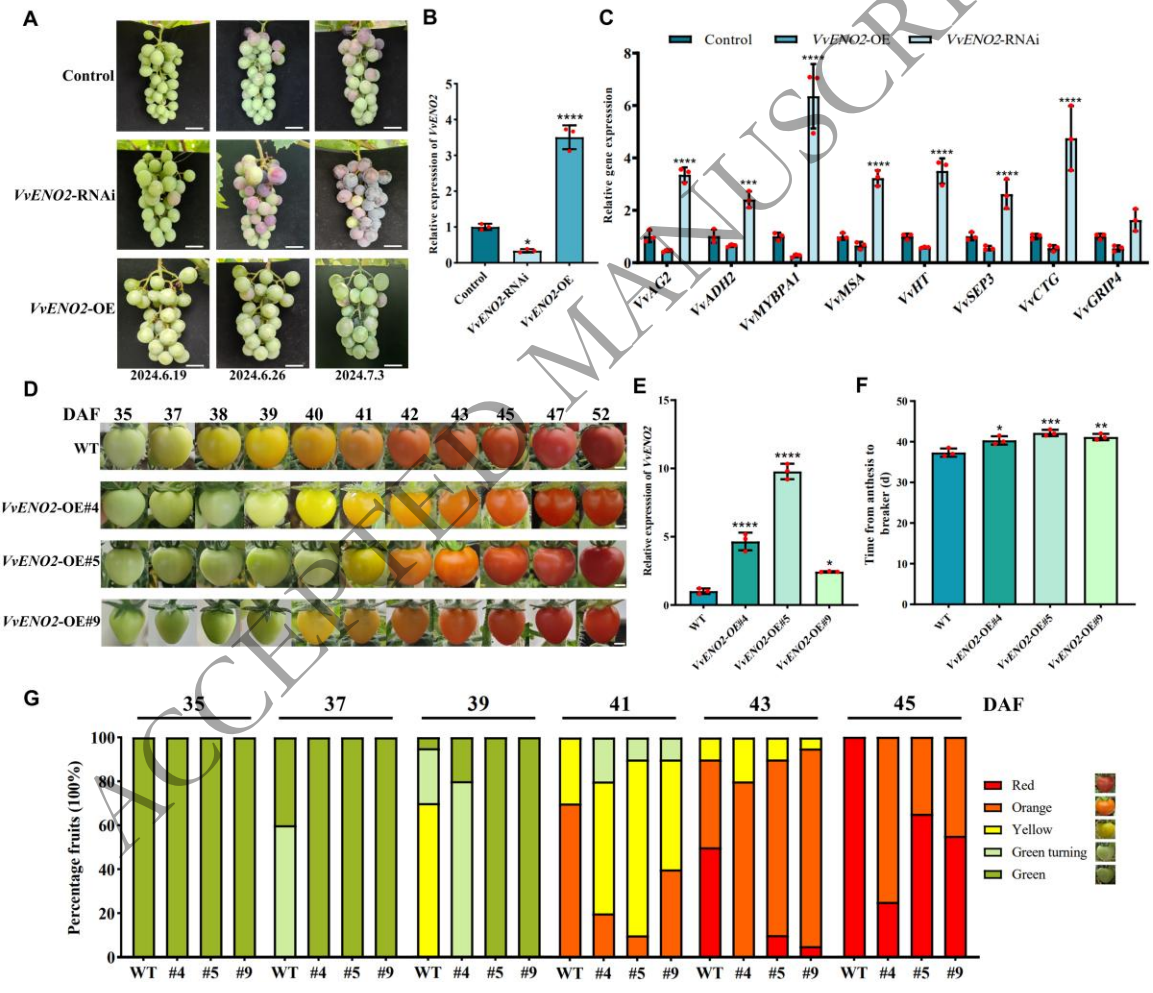


1047
1048

ACCEPTED MANUSCRIPT

Downloaded from academic.oup.com/hr/advance-article/doi/10.1093/hr/uhag485/9097232 by Bursa Uludag University user on 19 November 2026

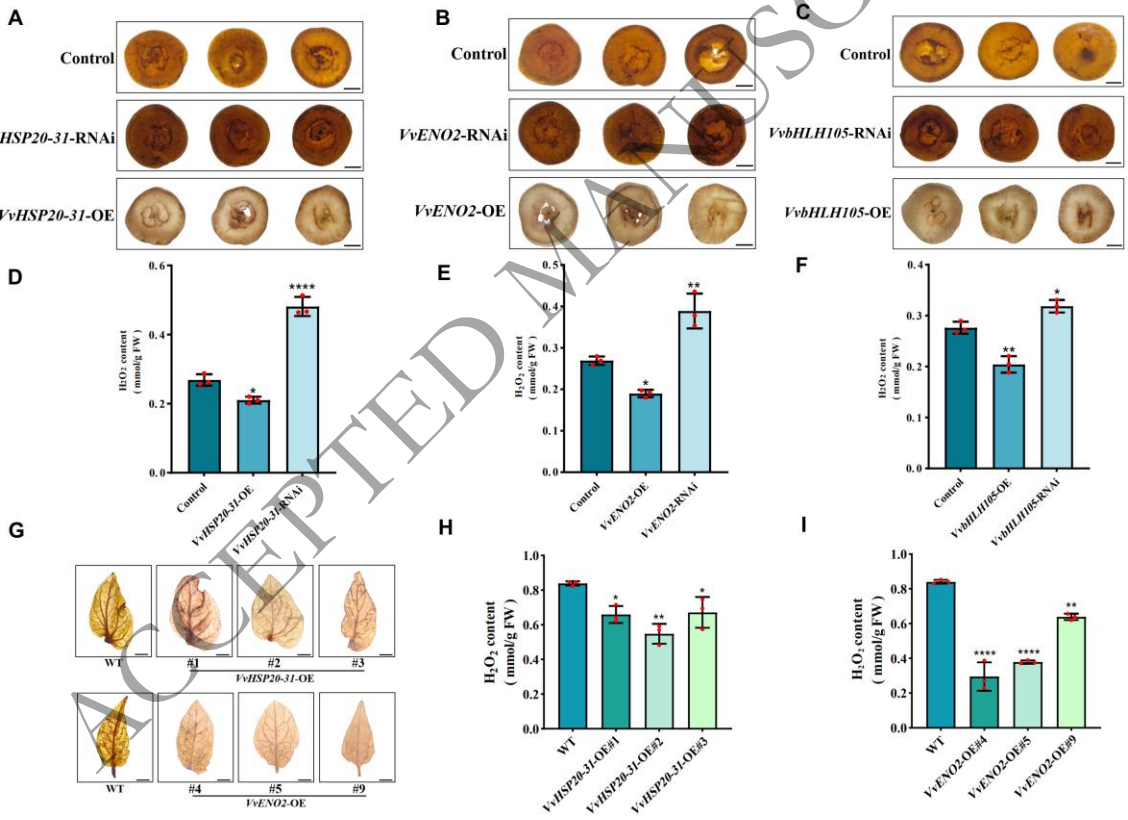
Figure 7 *VvENO2* negatively regulates fruit ripening. **(A)** Transient overexpression or silencing of *VvENO2* in grape berry phenotypes. The pIR empty was used as a control, and the scale bar was 1 cm. **(B)** RT-qPCR to detect the relative expression of *VvENO2*. **(C)** RT-qPCR to detect the expression of genes related to grape berry ripening. **(D)** Phenotypes of tomato fruits overexpressing *VvENO2*, the WT was used as a control, and the scale bar was 0.5 cm. **(E)** RT-qPCR to detect the relative expression of *VvENO2*. **(F)** Overexpressing *VvENO2* tomato fruit days from anthesis to color transition. **(G)** Percentage of fruit of each color stage for each line of tomato on the same day. Data are expressed as mean ± SD (n=3), the figures of (**B**), (**E**) and (**F**) were analyzed by one-way ANOVA, the figure of (**C**) was analyzed by two-way ANOVA, there were significant differences between the treatment group and the control group (*0.01<*P*<0.05, 0.001<**P*<0.01, 0.0001<***P*<0.001, ****P*<0.0001).



ACCEPTED MANUSCRIPT

Downloaded from academic.oup.com/hr/advance-article/doi/10.1093/hr/uhag485/9097232 by Bursa Uludag University user on 19 November 2026

Figure 8 DAB staining and H_2O_2 content determination of transiently transformed grape berries and transgenic tomatoes. **(A)** DAB staining of *VvHSP20-31* transgenic grape berry sections with pIR empty as control (scale bar, 1 cm). **(B)** *VvENO2* transgenic DAB staining of grape berry sections, the pIR empty as control (scale bar, 1 cm). **(C)** *VvbHLH105* transgenic DAB staining of grape berry sections, the pIR empty as control (scale bar, 1 cm). **(D)** H_2O_2 content determination of *VvHSP20-31* transgenic grape berry sections. **(E)** Determination of H_2O_2 content of *VvENO2* transgenic grape berry sections. **(F)** H_2O_2 content determination of *VvbHLH105* transgenic grape berry sections. **(G)** The DAB staining results for the *VvHSP20-31* and *VvENO2* transgenic tomato leaves, the WT as control. Scale bar, 1 cm. **(H)** The determination of H_2O_2 content in the *VvHSP20-31* transgenic tomato. **(I)** The determination of H_2O_2 content in the *VvENO2* transgenic tomato. Data are expressed as mean ± SD (n=3). FW is fresh weight, the figures of (**D**), (**E**), (**F**), (**H**) and (**I**) were analyzed by one-way ANOVA, there were significant differences between the treatment group and the control group (*0.01<*P*<0.05, 0.001<**P*<0.01, 0.0001<***P*<0.001, ****P*<0.0001).



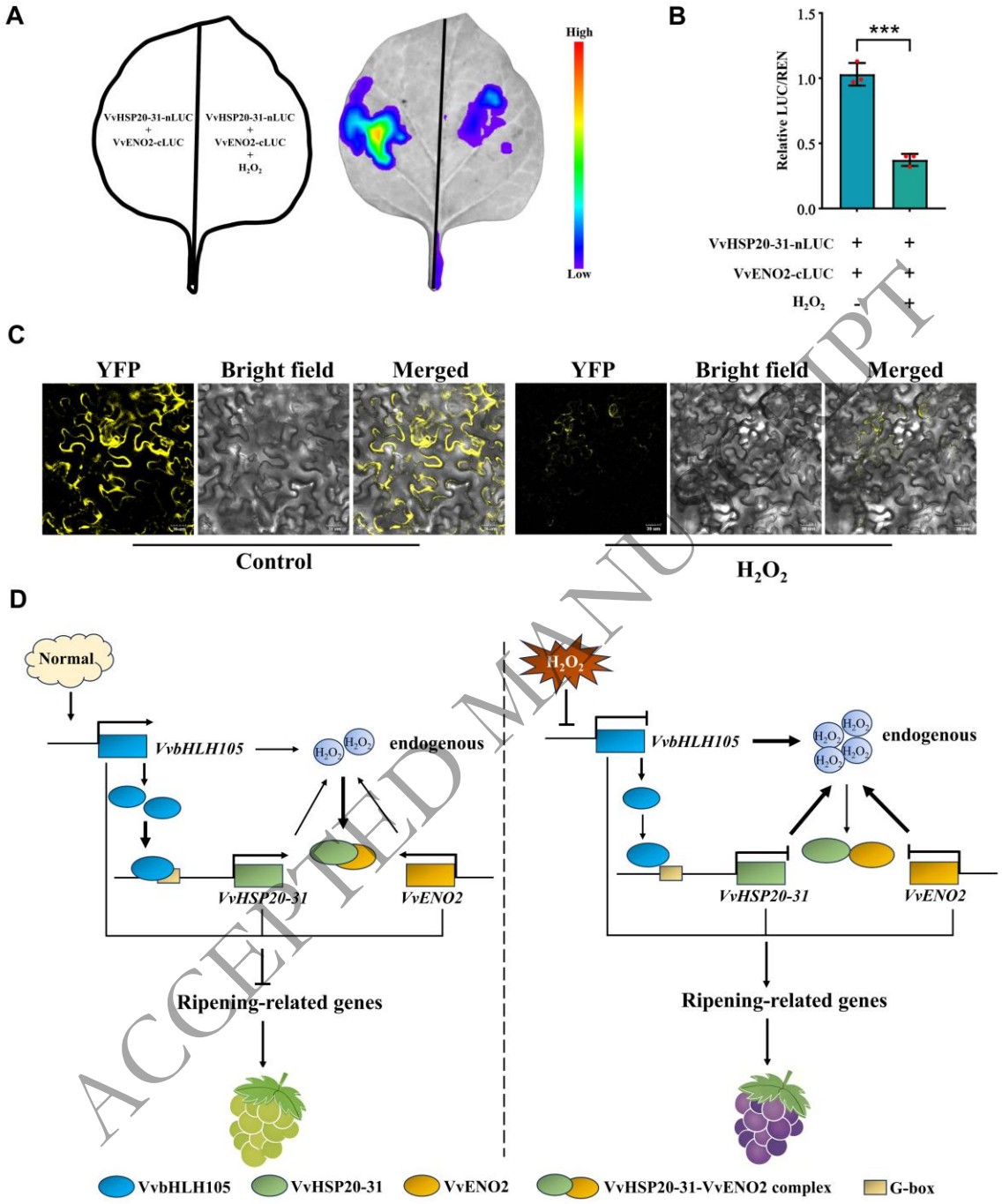
ACCEPTED MANUSCRIPT

Downloaded from academic.oup.com/hr/advance-article/doi/10.1093/hr/uhag485/9097232 by Bursa Uludag University user on 19 November 2026

Figure 9 H_2O_2 inhibited the interaction between VvHSP20-31 and VvENO2. **(A)** Live imaging revealed that VvHSP20-31 interacts with VvENO2 and is inhibited by H_2O_2. **(B)** Relative LUC activity assay of VvHSP20-31 interacting with VvENO2 and inhibited by H_2O_2. **(C)** BiFC analysis reveals that H_2O_2 attenuates the interaction between VvHSP20-31 and VvENO2. nYFP-VvHSP20-31+cYFP-VvENO2, untreated with H_2O_2, was used as a control, the scale bar of 30 μm. The figure of (**B**) was analyzed by t tests, different letters indicate significant differences (*0.01<*P*<0.05, 0.001<**P*<0.01, 0.0001<***P*<0.001, ****P*<0.0001), and data are presented as mean ± SD (n=3). The data undergoes normalization. **(D)** Model of the *VvbHLH105*/*VvHSP20-31*/*VvENO2* module in H_2O_2-mediated grape berry ripening. Under normal conditions, VvbHLH105 drives the transcription of *VvHSP20-31*. Elevated transcription of *VvbHLH105*, *VvHSP20-31*, and *VvENO2* reduce endogenous H_2O_2 content in berries, suppress the expression of berry ripening genes, thereby delaying ripening. Following exogenous H_2O_2 treatment, the promoter activity of *VvbHLH105* is suppressed, leading to a decrease in its transcription, which in turn results in reduced transcription of *VvHSP20-31*. Reduced transcription of *VvbHLH105, VvHSP20-31*, and *VvENO2* elevate endogenous H_2O_2 content in berries. This further inhibits the formation of the VvHSP20-31-VvENO2 complex while promoting the expression of berry ripening genes, ultimately accelerating ripening. Pointed arrows indicate activation. Flat arrows indicate inhibition.

ACCEPTED MANUSCRIPT

Downloaded from academic.oup.com/hr/advance-article/doi/10.1093/hr/uhag485/9097232 by Bursa Uludag University user on 19 November 2026



1096

ACCEPTED MANUSCRIPT

Downloaded from academic.oup.com/hr/advance-article/doi/10.1093/hr/uhag485/9097232 by Bursa Uludag University user on 19 November 2026